FORMATION OF LARGE REGULAR SATELLITES OF GIANT PLANETS IN AN EXTENDED GASEOUS NEBULA I: SUBNEBULA MODEL AND ACCRETION OF SATELLITES. I. Mosqueira, *NASA Ames Research Center/SETI, Moffett Field CA 94035, USA (mosqueir@cosmic.arc.nasa.gov)*, P. R. Estrada, *Cornell University, Ithaca CA 14853, USA, (estrada@astro.cornell.edu).*

We model the subnebulae of Jupiter and Saturn wherein satellite accretion took place. We expect a giant planet subnebula to be composed of an optically thick (given gaseous opacity) inner region inside of the planet's centrifugal radius (located at $r_c^J \sim 15R_J$ for Jupiter and $r_c^S \sim 22R_S$ for Saturn), and an optically thin, extended outer disk out to a fraction of the planet's Roche lobe, which we choose to be $\sim R_{roche}/5$ (located at $\sim 150R_J$ near the inner irregular satellites for Jupiter, and $\sim 200R_S$ near Phoebe for Saturn). This places Titan and Ganymede in the inner disk, Callisto and Iapetus in the outer disk, and Hyperion in the transition region. The inner disk is the leftover of the gas accreted by the protoplanet. The outer disk results from the solar torque on nebula gas flowing into the protoplanet during the time of giant planet gap opening (Bryden *et. al.* 1999). For the sake of specificity, we use a cosmic mixture "minimum mass" model to constrain the gas densities of the inner disks of Jupiter and Saturn (and also Uranus). For the total mass of the outer disk we use the simple scaling $M_{disk} \sim M_P \tau_{gap}/\tau_{acc}$, where M_P is the mass of the giant planet, τ_{gap} is the gap opening timescale, and τ_{acc} is the giant planet accretion time. This gives a total outer disk mass of $\sim 100M_{Callisto}$ for Jupiter and possibly $\sim 200M_{Iapetus}$ for Saturn (which contain enough condensables to form Callisto and Iapetus respectively). Our model has Ganymede at a subnebula temperature of ~ 250 K and Titan at ~ 100 K. The outer disks of Jupiter and Saturn have constant temperatures of 130 K and 90 K respectively.

This model has Callisto forming in a timescale $\sim 10^6$ years, Iapetus in $\sim 10^6 - 10^7$ years, Ganymede in $10^3 - 10^4$ years, and Titan in $10^4 - 10^5$ years. Callisto takes much longer to form than Ganymede because it draws materials from the extended, low density portion of the disk; its accretion timescale is set by the inward drift times of satellitesimals with sizes $300 - 500$ km from distances $\sim 100R_J$. This may be consistent with a partially differentiated Callisto with a $\sim$ 300 km clean ice outer shell overlying a mixed ice and rock-metal interior as suggested by Anderson *et al.* (2001). It is also possible that particulate matter coupled to the high specific angular momentum gas flowing through the gap after giant planet gap-opening lengthens the timescale for Callisto's formation. Furthermore, this model has Hyperion forming just outside Saturn's centrifugal radius, captured into resonance by proto-Titan in the presence of a strong gas density gradient as proposed by Lee and Peale (2000). While Titan may have taken significantly longer to form than Ganymede, it still formed fast enough that we would expect it to be fully differentiated. In this sense, it is more like Ganymede than like Callisto (Saturn's analog of Callisto, we expect, is Iapetus). An alternative *starved disk* model whose satellite accretion timescale for *all* the regular satellites is set by the feeding of planetesimals and/or gas from the planet's Roche-lobe implies a long accretion timescale for Titan with small quantities of NH_3 present, leading to a partially differentiated (Callisto-like) Titan. The Cassini mission is likely to resolve this issue conclusively. We briefly discuss the retention of elements more volatile than H_2O as well as other issues that may help to test our model.

1 Introduction

The large satellites of Jupiter and Saturn (the Galilean satellites plus Titan) generally have low inclinations and eccentricities. Perhaps most striking is the progression of satellite density in the Galilean system ($\rho_s = 3.5$ g cm^{-3} for Io, $\rho_s = 3.0$ g cm^{-3} for Europa, $\rho_s = 1.94$ g cm^{-3} for Ganymede, and $\rho_s = 1.85$ g cm^{-3} for Callisto). Furthermore, some characteristics of the regular satellite systems of the giant planets are quite similar (Pollack *et al.* 1991), in particular the ratios between the satellite systems and the parent bodies of mass, angular momentum, and size. These similarities suggest a common origin in an accretion disk present about the protoplanets at a late stage of their formation. These properties taken together with the tantalizing ratio of satellite to primary of $M_s/M_P \sim 10^{-4}$ (not too dissimilar from the ratio of giant planet to Sun) lead one to think of the Galilean satellite system as a kind of scaled-down solar system with the satellites accreting from a circumplanetary disk left over from the process of planetary formation.

An issue we wish to focus on is how to view Titan ($\rho_s = 1.88$ g cm^{-3}) in light of the Galilean satellite system. While Titan is located midway between Ganymede and Callisto in terms of planetary radii, scaled by the Hill radius of the primary the association is much closer to Ganymede. On the other hand, if the key quantity is the speed of incoming projectiles from the Roche-lobe then Titan can be thought of more as a Callisto with a thick atmosphere. Whatever the case, the similarities in distances, masses and densities of all three satellites lead us to attempt a detailed comparison between them.

As intriguing as the similarities are the differences between these three satellites. Ganymede is differentiated, while Callisto is only partly differentiated (Anderson *et al.* 1998) and shows no evidence of tectonic activity. On the other hand, the association of craters with the presence of CO_2 in Callisto but not Ganymede (Hibbits *et al.* 2000) as well as the breakdown of craters presumably due to the sublimation of CO_2 in Callisto but not Ganymede (Moore *et al.* 1999), which is consistent with the presence of a CO_2 atmosphere in Callisto (Carlson 1999), seems to require that Callisto be assembled

with and retain oxidized ices more volatile than H_2O. In the case of Titan, it is probably the presence of methane in the atmosphere that has received the most attention (Lunine *et al.* 1989; Prinn and Fegley 1989). Prinn and Fegley (1981) established that methane and ammonia were the dominant carbon-bearing and nitrogen-bearing molecules in the hypothesized Saturnian subnebula, provided that this disk was of solar composition, gaseous, optically thick and had access to regions close to Saturn with high ($\sim$ 800 K) quench temperature and 1 bar pressure. Such a disk is consistent with the subnebula model of Lunine and Stevenson (1982) or the spin-out scenario of Pollack *et al.* (1991).

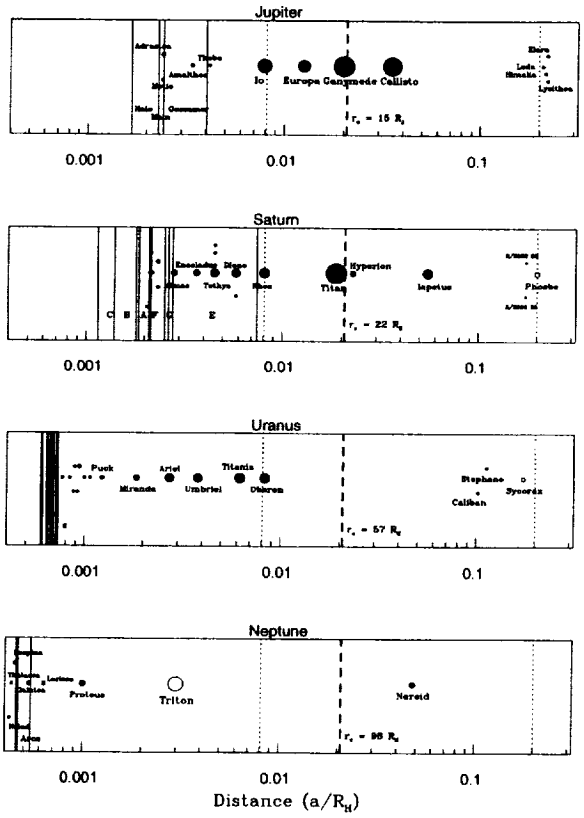

Figure 1: Comparison of the Jovian, Saturnian, and Uranian dynamical systems with the distance scale in terms of the respective planet's Hill radius ($R_H^J \sim 750R_J$, $R_H^S \sim 1100R_S$, $R_H^U \sim 2740R_U$). Planetary rings are denoted by solid lines, and are labeled when possible. The centrifugal radius is denoted by a bold dashed line. Dotted lines correspond to positions of interest. The first located at the distance of Rhea for Saturn, corresponds to the innermost portion of the disk. The second corresponds to the outer edge of the disk ($\sim R_{roche}/5$) in our models.

Another challenging problem is the result that the Galileo mission moment of inertia data are consistent with a fully differentiated Ganymede, but only a partially differentiated Callisto (Anderson *et al.* 1998). More recently, Anderson *et al.* (2001) have investigated two and three layer models for Callisto's internal structure assuming hydrostatic equilibrium. For the two layer models these authors find two limiting cases: a relatively pure ice shell about $\sim$ 300 km overlying a mixed ice and rock-metal interior, and a thick $\gtrsim$ 1000 km ice and rock-metal outer shell overlying a rock-metal core. Since it is difficult to reconcile a metallic core with a partially differentiated state the former solution appears more likely. Given that accreting bodies allocate a fraction of their energy as surface heat (Schubert *et al.* 1981; Coradini *et al.* 1982), fast satellite accretion would melt the water ice and lead to rock separation and runaway differentiation (Friedson and Stevenson 1983). Since a differentiated depth of $\sim$ 300 km may trigger this mechanism, Anderson *et al.* (2001) suggest that Callisto may be in the process of differentiating, only it is doing so slowly. Previous attempts to explain an undifferentiated Callisto have relied on fine tuning parameters (Schubert *et al.* 1981; Coradini *et al.* 1982; Lunine and Stevenson 1982). While it is possible that non-hydrostatic effects in Callisto's core could be large enough to allow for complete differentiation of Callisto and sufficiently small in Ganymede to avoid detection, we regard this possibility as unlikely. Instead, we favor a model that makes Callisto slowly.

Other issues also seem difficult to explain. For instance, one might expect the outermost Galilean satellite to have significantly less angular momentum than the preceding satellite. If we insist in forming all the Galilean satellites out of a more or less uniform accretion disk, the size of Callisto would seem to require a disk with a very sharp outer cut-off outside Callisto. It seems unlikely that the satellite disk would have enough surface density to make a satellite the size of Callisto at $26R_J$, but form no smaller objects further out. Furthermore, the separation between Ganymede and Callisto ($\sim 10R_J$) is so large that one is led to wonder why there are no satellites in between at $\sim 20R_J$. One can imagine that the inner three satellites evolved inward from their original positions, but then Callisto should also have evolved (evolution outward due to tidal effects does not help with this issue). On the other hand, one can always argue serendipity, but the Galilean satellite system is sufficiently regular that we reserve this explanation as a last resort.

A similar point can be made concerning Titan and Iapetus. If we form the satellites out of a continuous, smoothly varying accretion disk, it would seem difficult to explain why there are no large satellites between Titan at $20R_S$ and Iapetus at $60R_S$ (Hyperion does not have enough mass to affect this argument). Finding an explanation for the observations concerning the bulk properties of the regular satellites of the giant planets is made even more difficult when one considers that the Saturnian satellite system is so different from the Jovian satellite system. Perhaps the most perverse difference between the two systems is the fact that whereas the Galilean satellites get rockier closer to the planet, the inner satellites of Saturn appear to be made mostly of ice! Even so, we attempt a combined model for both Jupiter and Saturn (as well as Uranus).

If we take the satellite systems of Jupiter and Saturn and

add the amount of gas necessary to create a cosmic composition mixture the resulting disks have a total angular momentum comparable to the spin angular momentum of the parent planet (Stevenson *et al.* 1986). This is consistent with the spin-out scenario (Korycansky *et al.* 1991) which suggests that giant protoplanets shed gas as they contracted. The issue arises whether one would expect the circumplanetary disk to exhibit a solar mixture of elemental abundances of water and ice bearing materials. While one can think of several processes which modified the abundances of rock and ice from their solar abundances. Yet, the fact that the similarly sized Ganymede, Callisto and Titan all deviate from solar mixture by the same proportion ($\sim$ 60 % rock, $\sim$ 40 % ice by mass; though Triton, Pluto and Charon all have a considerably higher silicate fraction) seems to indicate that one should be guided by solar mixtures and investigate mechanisms for deviation from them, such as size-dependent water vaporization on one end, and water enrichment by composition selective mechanisms on the other. If so, one might calculate models with "minimum mass" by augmenting the mass of the satellites by some factor (typically $\sim$ 100), corresponding to the mass ratio of gas to rock/ice in the solar nebula. This factor might be decreased somewhat in view of the heavy-element enrichment of the giant planets, or increased in view of the possible loss of some of the accreting materials as a result of the specifics of the process used to make the planet and satellites. Given the uncertainty inherent in these arguments, and the lack of observational evidence of wide systematic departures from solar mixtures, it is reasonable to continue to use solar proportions as a guide. Furthermore, we regard the order of magnitude agreement between protoplanetary disk models (Lunine and Stevenson 1982) and the "minimum mass" model as suggestive that one should indeed expect close to solar mixtures in the circumplanetary disk.

In order to arrive at a specific model for the formation of regular satellites in a gaseous medium we need to characterize the subnebular viscosity. It has been suggested that because of the stabilizing influence of a positive radial gradient in specific angular momentum, turbulence in a Keplerian disk is not self-sustaining unless a source of "stirring" is found (Ryu and Goodman 1992; Balbus, Hawley and Stone 1996). As a result, one needs to identify a specific mechanism that can maintain turbulence in the dense, high orbital frequency subnebula. One such suggestion is that convection drives turbulence (Lin and Papaloizou 1980; Ruden and Lin 1986); however, eventually particle growth stops convection by diminishing the Rosseland mean opacity and weakening its temperature dependence (Weidenschilling and Cuzzi 1993). Given the fast dynamical timescale and the high particle density of the subnebula disk, coagulation and settling times for sticky particles is likely to take place on a timescale considerably faster than disk evolution. Thus, convection probably cannot drive disk evolution. Another possibility is that turbulence is driven by a magneto-hydrodynamic (MHD) instability (Balbus and Hawley 1991). But this is also unlikely to apply (Gammie 1996) in the dense, dusty and relatively cool subnebula disk. Alternately, there are a variety of ways that accretion itself, or the gravitational energy released by it, can provide the source of free energy that can drive turbulence. It has been pointed out (but not quantitatively explored) that a turbulent shear layer where the angular momentum of the infalling gas is adjusted to the angular momentum of the Keplerian disk flow exists below an accretion shock and may provide a localized viscosity (Cassen and Moosman 1981; Cassen and Summers 1983). More recently it has been shown that a bump in the temperature profile of the disk, as may result from accretion, leads to Rossby waves and localized turbulence (Lovelace *et al.* 1999; Li *et al* 2000). Similarly but more generally, Klahr and Bodenheimer (in press) study a global baroclinic instability as a source of turbulence and angular momentum transport in Keplerian accretion disks characterized by a negative entropy gradient. Such a model leads to turbulence that is a function of position and time.

In order to create a coherent scenario of satellite formation, the source of the solids that go into the satellite systems must be considered. It is possible that the concentration of rock/ice to gas in the subnebula depends on the ability of the protoplanet to disturb the orbits of planetesimals situated within a few AU of its orbit into ones that crossed its orbit (Gladman *et al* 1990). One would expect that within a timescale much shorter than the lifetime of the solar system virtually all the planetesimals located in the outer solar system would have their orbits perturbed into giant planet crossing orbits. What happens to such a planetesimal depends on the size of the planet at the time of crossing. If the giant planet's envelope filled a fair fraction of its Hill radius (as it probably did during all or most of the later stages of accretion, unless significant amounts of gas accreted through the gap) then planetesimals < 100 km (Zahnle, private communication) may break up high in the contracting envelope of the giant planet, and be left behind with the gas disk. Late arriving planetesimals might have been scattered to further out regions of the solar system with some sent to the Oort cloud and some lost altogether. Our model relies on early arriving planetesimals that breakup in the extended Jovian and Saturnian envelopes to provide the bulk of the material that will eventually make the satellite systems. This model is consistent with a model that forms the irregular satellites of Jupiter at a time when the proto-planetary envelope was collapsing rapidly and extended several hundred planetary radii (Pollack *et al.* 1979). The idea is for the envelope to capture objects into planetary orbits yet not drag them into the planet. A similar model might apply to the capture of Phoebe in orbit around Saturn. In this model late arriving interplanetary debris plays a role in that it can threaten the survival of regular satellites close to their primary. Thus, the large disparity in masses between Titan and all other moons of Saturn may be the result of breakup of satellites by high-velocity impacts (Lissauer 1995). In this model, it is also possible that the outermost large, regular moon in the Jovian and Saturnian systems, which is located outside the centrifugal radius, derives a fraction of its mass from particulate matter coupled to the high specific angular momentum gas flowing through the gap after gap-opening, once the giant planet has accreted most of its mass. By contrast, a *starved disk* model (Stevenson 2001) relies on the late arriving planetesimals and/or flow through the gap to form a disk around

the planet out of which *all* the regular satellites will eventually accrete. One must keep in mind, however, that most planetesimals were probably scattered or the giant planets would have ended up with too much high-Z mass (Podolak *et al.* 1993), and that most of the mass in the disk at late times is in the form of planetesimals (Weidenschilling 1997). Furthermore, gas arriving at late times may have sufficient specific angular momentum to place it in orbit outside of the centrifugal radius (whereas most of the mass in the satellite systems of the giant planets is inside of this radius).

TABLE I
Satellite Data[a]

	Distance (R_P)	Radius (km)	Density (g cm^{-3})	Mass (10^{26} g)
Jupiter	1.0	71492	1.326	18980
Io	5.905	1,821	3.53	0.894
Europa	9.937	1,565	2.97	0.480
Ganymede	14.99	2,634	1.94	1.4823
Callisto	26.37	2,403	1.85	1.0776
(Leda)	155.2	5	?	?
(Himalia)	160.6	85	?	?
(Lysithea)	163.9	12	?	?
(Elara)	164.2	40	?	?
Saturn	1.0	60330	0.687	5684.6
Mimas	3.075	199	1.12	0.00037
Enceladus	3.945	249	1.00	0.00065
Tethys	4.884	529	0.98	0.0061
Dione	6.256	560	1.49	0.011
Rhea	8.736	764	1.24	0.023
Titan	20.25	2,575	1.88	1.3457
Iapetus	59.03	720	1.0	0.016
(S/2000 S5)[b]	187.3	10	?	?
(S/2000 S6)[b]	189	16	?	?
(Phoebe)	214.5	115x105	?	?
Uranus	1.0	25559	1.318	868.32
Puck	3.36	77	?	?
Miranda	5.08	240x233	1.20	0.000659
Ariel	7.48	581x578	1.67	0.0135
Umbriel	10.4	585	1.4	0.0117
Titania	17.05	790	1.71	0.0353
Oberon	22.8	760	1.63	0.0301
(Caliban)	280.5	30	?	?
(Stephano)[b]	309	10	?	?
(Sycorax)	477.9	60	?	?
Neptune	1.0	24766	1.638	1024.3
Proteus	4.75	218x201	?	?
(Triton)	14.32	1,353	2.05	0.215
Nereid	222.6	170	?	?

[a] From *TheNewSolarSystem*, J. K. Beatty, Ed. (1999)
[b] P. Nicholson, private communication

In section 2 we organize the satellite systems of the giant planets according to the Hill radius of the primary. In section 3 we characterize the subnebulae of giant planets, especially that of Jupiter. In section 4 we discuss the accretion of the Galilean satellites, reserving discussion of Callisto for Section 5. In section 6 we turn to Saturn's satellite system. In section 7 we discuss the satellite system of Uranus. In section 8 we make some comments on an alternative satellite accretion model which leads to a long accretion timescale for every satellite. In section 9 we present our conclusions and discussion. In Mosqueira and Estrada (2002, submitted to Icarus, hereafter Paper II) we turn to the migration and survival of full-sized satellites.

2 Regular Satellites of Giant Planets

We start with a brief comparative discussion of the satellite systems of the giant planets. Here we advance arguments discussed in the remainder of the paper so as to organize the systems under consideration, and facilitate the ensuing discussion.

Proper comparison of the satellites requires we establish a guiding principle to order the satellite systems. We believe satellite positions should be compared in terms of the Hill radius $R_H = a(M_P/3M_\odot)^{1/3}$ of the primary (and the concomitant centrifugal radius $r_c \approx R_H/48$). In **Figure 1**, we plot the locations of the regular satellites (solid circles) and the innermost irregular satellites (open circles) in units of the Hill radius of the giant planet. The bold dashed line describes the position of the centrifugal radius. From this plot it is immediately apparent that the irregulars (presumed to be captured objects) for the three inner giant planets are far from the location of the centrifugal radius. We expect that this observation means that the gas disk which gave rise to the regular satellite systems extended well outside this radius ($\sim R_H/5$ for Jupiter and Saturn). Jupiter and Saturn have regular satellites which are far outside the centrifugal radius, with Saturn's Iapetus being much further out than Jupiter's Callisto. These two planets also have satellites just inside (Saturn also just outside) the centrifugal radius. By contrast, one has to go much deeper in ($\sim R_H/100$) to find any regular Uranian satellites. For this planet we expect that the location of irregulars closer to centrifugal radius is related to the absence of a regular satellite outside of this radius.

We add the satellite system of Neptune for the sake of completeness; however, Goldreich *et al.* (1989) showed that retrograde Triton is likely to be a captured object. Since these authors estimate a collision probability near one between $\sim 5R_N$ and the centrifugal radius $\sim 100R_N$, Triton's capture would have broken up or scattered any pre-existing satellites in this region. Nereid's high eccentricity and inclination, and large semi-major axis are best understood in terms of this process. Hence we will not discuss this system any further. We provide data on both regular and irregular satellites for all four giant planets in **Table I**.

3 The Giant Planet Subnebula

The "minimum" mass subnebula we use here is one of solar nebula composition that provides just enough mass to form the observed satellite systems with the observed rock/ice mass ratio. Given Jupiter's relative enrichment in heavy elements with respect to the solar nebula, the "minimum" mass subnebula is not a firm lower bound. On the other hand, inefficiencies in the satellite formation process and depletion of solids due to planetesimal formation mean that it is not a firm upper bound either. Still it remains a useful reference and we have chosen it for the sake of specificity. As we will see, it is possible that a minimum mass subnebula (unlike the minimum mass solar nebula) does in fact apply. If anything, we expect that the concentration of solids will turn out to be larger than solar proportion. Here and in paper II we will be guided by solar proportion, but we will also consider solid enhancement factors of $3-4$ in rough agreement with giant planet high-Z enhancement.

Gas flowing into the Hill sphere forms a high optical depth gas disk around the protoplanet. We can obtain an estimate of the size of this disk by assuming that gas elements conserve specific angular momentum once they enter the planet's Hill sphere. Equating the centrifugal radius to the planetary gravitational forces, one obtain the centrifugal radius $r_c \approx R_H/48$ (Cassen and Pettibone 1976; Stevenson *et al.* 1986). For Jupiter and Saturn these are $r_c^J \approx 15R_J$ and $r_c^S \approx 22R_S$ respectively, remarkably close to the positions of Ganymede and Titan. It is tempting to conclude that this is roughly the size of the gas disk which led to formation of the satellites. One must keep in mind, however, that Callisto is at $26R_J$ nearly twice the size of Jupiter's centrifugal radius, and Iapetus is at $59R_S$ nearly three times the size of Saturn's centrifugal radius. Our model accounts for these facts by using a two component protoplanetary subnebula. As the planet grows the centrifugal radius moves outward. Since the giant planet accretion timescale may be comparable to the viscous evolution timescale a thick inner disk forms. Inside of the centrifugal radius (after planetary accretion has been completed) the average surface gas density Σ exceeds 10^5 g cm^{-2}, which yields a vertical optical depth (not including ice grains) due to absorption by hydrogen molecules $\tau_v \sim \Sigma K_{gas} \sim 10$, where $K_{gas} \sim 10^{-4}$ cm^2 g^{-1} is the Rosseland mean gas opacity (Lunine and Stevenson 1982). Well outside the centrifugal radius gas surface densities are in the range $10^2 - 10^3$ g cm^{-2}, which results in a low vertical optical depth in the range $\tau_v \sim 0.01 - 0.1$. As we shall see, this transition from high optical depth to low optical depth has important consequences when it comes to the temperature profile, the turbulence properties of the subnebula, as well as for the process of satellite formation itself.

While grains increase the opacity so long as grain sizes are in the order of the infrared wavelength, we expect that coagulation will quickly lead to larger grain sizes (Weidenschilling and Cuzzi 1993). In the subnebula we expect that the dust density is determined by a balance between the collisional dust production rate and the removal rate by drift, coagulation, accretion and the like. In such an equilibrium state it may be appropriate to assume a power law size distribution. If we take this distribution to behave like r_p^{-3} (as may result in a collisional situation where erosion replenishes small particles) and use $r_p = 10^3$ cm as the upper size cut-off, we find that the mass in particles smaller than μm is $\sim 10^{-7}$ of the total mass in the disk. Using $\Sigma_s = (4/3)\rho_s r_p \tau_{dust}$, where τ_{dust} is the micron-sized dust optical depth, we find that for disk surface densities $\Sigma_s < 10^3$ g cm^{-2} we have $\tau_{dust} < 1$ (where a grain density of $\rho_s = 1.0$ g cm^{-3} has been used). As a result, the dust optical depth is likely to drop below 1 once the satellites have accreted (in a starved disk, where the disk surface density is always small, the dust optical depth may always be < 1). However, the possibility that close to the planet hypervelocity collisions lead to large dust production and dust optical depth > 1 cannot be ruled out. We return to this issue in Paper II. For now we simply consider the gaseous opacity alone.

If the opacity is small, individual grains are in radiative balance with the planet's luminosity and heat the surrounding gas and a temperature profile results with $T \propto r^{-1/2}$ (Pollack *et al.* 1977) (though some intricacies, which we need not get into here, result in "flaring" disks [e.g. Chiang and Goldreich 1999]). On the other hand, when the opacity is high, viscous dissipation within the nebula plays a central role in heating the gas and driving its evolution (Lynden-Bell and Pringle 1974). Lin and Papaloizou (1980) and Lin (1981) have suggested that thermal convection in the vertical direction drives the turbulence that leads to viscous dissipation, and have used mixing length theory to calculate it. According to their models, the inner opaque regions of viscous accretion disks have a temperature profile given by $T \propto r^{-3/2}$; however, rapid particle coagulation means that it is unlikely that convection drives turbulence in the Jovian subnebula. Klahr and Bodenheimer (2001) show that a radial entropy gradient can lead to strong global turbulence. Such a radial gradient is likely to apply to the non-isothermal optically-thick portion of the subnebula gas disk, and it may lead to a temperature profile of the form $T \propto r^{-1}$ as is suggested by some solar nebula models (Cameron and Pine 1973; Cameron 1978). Like previous authors (Lewis 1972; Lunine and Stevenson 1982), we characterize the temperature of the gas disk by choosing the current radial distance for Ganymede as the location for the condensation of ice.

There are numerous processes at work that might conceivably lead to satellite migration. Most importantly, the gas torque on a full-sized Galilean satellite, when most of its water was already accreted, may alter the appropriate choice for the location of the condensation of ice. Nevertheless, the closeness of Ganymede to Jupiter's centrifugal radius tends to make us think that this satellite underwent limited radial migration. Furthermore, our model makes Ganymede from materials accreted by gas drag between $\sim 15R_J$ to $\sim 23R_J$. Thus, setting the ice condensation temperature at $15R_J$ ensures that nearly all of the material that went into Ganymede had its complement of water in place. The resulting temperature profile is $T = 3600/x$, where $x = r/R_J$, which is the same profile as that chosen by Lunine and Stevenson (1982); however, unlike that work, which formed all the Galilean satellites out of a

dense subnebula, in our model the high-optical depth subnebula extends only out to $\sim 25R_J$, which does not encompass Callisto's radial location.

It should also be noted that the inner disk is not isothermal in the vertical direction. We expect that the temperature at the midplane is several times the temperature at the disk surfaces. Therefore, the above temperature represents a vertically averaged quantity. In the outer disk the temperature can be as low as the solar nebula temperature at the location of Jupiter $\sim$ 130 K. For times $\sim 10^7$ years, after accretion, once the planet has had a chance to cool, the temperature in the disk is constant and equal to the background temperature.

There are three mechanisms that can lead to the presence of an extended gas disk. The giant planet can spin-out a disk during its contraction phase (Korycansky *et al.* 1991). In a viscous disk, gas inside the radius of maximum viscous stress (probably located in the neighborhood of the centrifugal radius) drifts inwards as it loses angular momentum while gas outside this location expands outwards as it receives angular momentum (Lynden-Bell and Pringle 1974). Finally an extended disk will result from the torque of the Sun on gas flowing from the Roche-lobe. In this study we favor the latter possibility. In order to characterize the properties of the extended, low density disk outside the centrifugal radius we make use of simple scaling relations. Numerical studies show that after Jupiter opens a gap in the solar nebula a large disk of circumplanetary gas is left (Bryden *et al.* 1999; Korycansky and Papaloizou 1996). The argument presented here is based on angular momentum calculations where the size of the disk is determined by the torque of the Sun on the infalling gas (Bryden *et al.* 1999).

It is useful here to discuss planetary gap opening in some detail. We can estimate the timescale for gap opening by calculating the angular momentum L_Δ in an annulus of half-width Δ. Given the planetary torque on this annulus $\dot{L}_T$, the timescale for gap opening is given by $\tau_{gap} \approx L_\Delta/\dot{L}_T$. An analytical estimate for the gap opening timescale can be obtained using the torque formula (Lin and Papaloizou 1993)

$$\dot{L}_T = 0.23 \left(\frac{M_P}{M_\odot}\right)^2 \Sigma a_P^4 \Omega^2 \left(\frac{a_P}{\Delta}\right)^3, \qquad (1)$$

where the planetary feeding zone Δ must be larger than the scale-height of the nebula H at the semi-major axis of the giant planet a_P. The angular momentum the planet must remove from the annulus of half-width Δ in order to open up a gap is approximately given by

$$\begin{aligned} L_\Delta &\approx M(GM_\odot)^{1/2}((a_P+\Delta)^{1/2} - (a_P + \frac{1}{2}\Delta)^{1/2}) \\ &\approx \frac{1}{4} M\Omega a_P \Delta, \end{aligned} \qquad (2)$$

where $M = 2\pi\Sigma\Delta a_P$ so that $L_\Delta \approx \frac{1}{2}\pi\Sigma\Omega a_P^2\Delta^2$. Then we have the gap opening time $\tau_{gap} \approx (\Delta/a_P)^5 P/q^2$, where $q = M_P/M_\odot$ (Bryden *et al.* 1999). Unless Δ is several times the planet's Hill radius, accretion onto the planet will continue. For some nebula models (Lubow *et al.* 1999) a gap will fail to stop the accretion of a Jupiter mass ($1M_J$) giant planet. These workers estimate that it will take a $6M_J$ planet to create a gap large enough with respect to its Roche-lobe to stop accretion onto the planet. Of course, it then becomes difficult to explain the mass of Jupiter. Nevertheless, gas flowing through the gap is clearly a significant issue that needs to be addressed. In our model, given its high specific angular momentum, this late arriving component simply adds gas and some condensables (what fraction of condensables is uncertain, though it is likely to be well below solar mixtures since at late times most of the solids are in the form of planetesimals which do not couple to the gas [Weidenschilling 1997]) to the outer disk after Jupiter has already accreted most of its mass. In any case, it is clear that the relevant size of the annulus Δ has to be large compared to the Roche-lobe of the planet in order to lower the mass rate accreted onto the planet. Using $\Delta \sim 0.2a_J$ (which is about three times larger than the Hill radius for Jupiter), we obtain $\tau_{gap} \sim 380P$, where P is the period of Jupiter's orbit. This estimate is similar to the numerical value $\tau_{gap} \sim 320\,P \sim 4 \times 10^3$ years given by Bryden *et al.* (1999).

It must be stressed that in the context of the satellites we are more interested in halting inward migration than we are in ending accretion. We expect accretion of the large, regular satellites to end when the disk has been depleted of condensables, or when an outer satellite limits the inner satellite's supply of inward drifting satellitesimals (see Section 4). This differs from the solar nebula context where a minimum mass model may not apply (Lissauer and Stewart 1993). It is possible, however, that gap-opening also plays a role in regulating the growth of satellites.

To obtain an estimate for the total mass left in the circumjovian disk after gap opening we use $M_{disk} \sim M_J\tau_{gap}/\tau_{acc} \sim 100\,M_{Callisto}$, where $\tau_{acc} \sim 10^6$ years is the timescale for the accretion of gas onto Jupiter. This estimate is meant to indicate that faster planetary accretion may lead to a larger outer disk mass. Using a mass ratio of gas to solids of $\sim$ 100 (Pollack *et al.* 1994), we obtain a mass of solids $\sim M_{Callisto}$. Determining the size of the outer disk requires careful calculation of the angular momentum of infalling material. Because the material flows in from the Roche-lobe, the angular momentum of the resulting disk is sensitive to the solar torque. Numerical simulations give sizes as large as $\sim R_{roche}/2$ (Bryden *et al.* 1999; Korycansky and Papaloizou 1996; Korycansky *et al.* 1991.) Thus, to the extent that we can apply solar composition mixtures to the Jovian subnebula, we expect that the outer gas disk extends to a fraction of the planet's Roche-lobe and contains enough rock/ice to form a Callisto-sized object. Here we adopt the more conservative choice $R_{roche}/5 \sim 150R_J$ for the size of the outer disk (we choose the same fraction for Saturn, which corresponds to a larger distance $\sim 200R_S$). We justify this choice by noting that the inner irregular Jovian satellites are located at $160R_J$ just outside this distance. That is, we tie the position of the outer disk to the location of the inner irregular satellites. Too much gas beyond this point

would have resulted in the inward drag of these objects. In our model, gas drag explains the absence of irregular satellites closer in to Jupiter (in the case of Saturn a similar argument can be made for Phoebe at $215R_S$). We expect that the same overall process that led to capture of the irregular satellites also yielded the bulk of the mass that ended up in the satellite systems. That is, prior to hydrodynamical collapse Jupiter's envelope extended out to $\sim 300R_J$ and led to the capture of irregulars inside of this radius (Pollack *et al.* 1979). After hydrodynamical collapse a disk was left behind that dragged in all the solids left in orbits $< 150R_J$. Even if a different method were employed to capture at least some of the irregular satellites, we stress that their locations imply a relatively sharp cut off in the gas distribution of the outer disk. This is difficult to reconcile with a viscous medium. We attribute this observation to the low viscosity of the gas in the optically thin, outer disk.

Even though our scenario is generally consistent with the spin out scenario of Korycansky *et al.* (1991), we do not rely on its validity. The spin out model assumes opacities that are arguably too large if one takes into consideration coagulation and settling of dust grains (which provide the source of the opacity). For lower opacities, the spin out would not have taken place. On a related issue, lower opacities would also lead to faster formation times for the giant planets. For instance, a Jupiter formation model with 2 % of the grain opacity of standard models would shorten Jupiter's accretion time from $\sim 7 \times 10^6$ years to $\sim 3 \times 10^6$ years (Olenka Hubickyj, private communication). Such a scenario would also invalidate the spin out results. Yet, our simple scaling formula for the mass of the outer disk shows that shorter planetary accretion times correspond to larger outer disk masses. It is worth noting that whether due to the Sun's torque on the infalling gas or the spin out of the protoplanetary envelope an extended disk will result. Since it seems likely that the opacity of the planetary envelope will decrease sharply as a result of the processes mentioned above, we favor a model that does not rely on the spin-out of the gaseous envelope.

So far we have described a circumplanetary disk (or subnebula) with an optically thick (even when grains are excluded) inner region inside of the centrifugal radius, and an optically thin outer region outside of the centrifugal radius and extending to a significant fraction of the Roche lobe. To characterize the transition region between the inner and outer disks let us first assume that planetary accretion drives subnebula turbulence. If we choose a timescale for gas evolution in the presence of accretion driven turbulent viscosity to be the gap opening time $t_0 \sim 1000$ years and we use a lengthscale on the order of the centrifugal radius $R_0 \sim r_c \sim 15R_J$, we get $\nu = R_0^2/t_0 \sim 10^{11} - 10^{12}$ cm^2 s^{-1}. This gives $\alpha \sim 10^{-4} - 10^{-3}$, consistent with the scenario of Klahr and Bodenheimer (2001). This leads us to expect that following planetary accretion the location of the gas density drop-off will be outside but close to the location of the centrifugal radius. Unfortunately, the size of the transition region is unknown. However, it must be larger than the scale-height to avoid becoming Rayleigh unstable (Lin and Papaloizou 1993). This sets our choice for the maximum surface density gradient in the transition region.

TABLE II
Surface Density Parameters

	Jupiter	Saturn (3.7)	Saturn (Iap)	Uranus
Σ_{in}^{0} †	51	10	11	1
Σ_{out}^{0} †	0.31	0.065	0.0077	?
$r_1^{\ddagger}$	20	25	25	57
$r_2^{\ddagger}$	26	37	41	?
$R_{in}^{\ddagger}$	14	16	18	?
$R_{out}^{\ddagger}$	87	115	117	?
$a_1^{\dagger}$	36	5.4	5.8	?
b_1^{*}	13	9	14	?

† Units are in 10^4 g cm^{-2}.

‡ Units are in planetary radii R_P.

* Unsmoothed values. $b_1 = \frac{\ln[(\Sigma_{in}^0 R_{in} r_2)/(\Sigma_{out}^0 R_{out} r_1)]}{\ln(r_2/r_1)}$.

Following the completion of accretion, the gas turbulence will significantly die down and the subnebula disk will cool in a Kelvin-Helmholtz timescale $\sim 10^4$ years (Stevenson *et al* 1986). At the outer edge of the inner disk, where the subnebula temperature approaches the background temperature of the solar nebula, the flow will become laminar, with very low viscosity and long evolution times. Closer in, remnant turbulence will be driven by the entropy gradient due to the planetary gravitational energy release. It can be seen that our model has a constant value for H/r inside of Ganymede. For such a model the entropy is a function of radial location $S(r) = p/\rho^{\gamma} \propto r^{-3+2\gamma}$, where p is the pressure, ρ is the mass density, and γ is the ratio of specific heats. Because the entropy decreases with distance, it gives rise to a non-zero baroclinic term (Klahr and Bodenheimer 2001). If we estimate the post-accretion turbulence inside Ganymede to be $\alpha \sim 10^{-5} - 10^{-6}$ then the timescale for Jupiter's inner disk to become optically thin is $\sim 10^4 - 10^6$ years, considerably shorter than the timescale for Jupiter to cool off in $\sim 10^7$ years. Thus, we expect the inner disk to continue evolving until a gas density of $\sim 10^4$ g cm^{-2} is reached. At that time the inner disk will become optically thin and the turbulence should die down. Hence it should be difficult to lower the density of the disk below gaseous optical depth of order unity by gas turbulence alone (unless small dust particles are kept around on viscous timescales, which presents a problem given the much shorter coagulation timescales). Once the planet cools down the subnebula will become essentially quiescent. In the low optical depth regions of the disk we have constant T and $S(r) \propto r^{\frac{5}{2}(\gamma-1)}$. For an isothermal gas $\gamma = 1$, so the entropy is constant. As a result, for the outer disk early on we expect weak turbulence close to the midplane driven by the presence of a dust and rubble layer (due to the particle shear layer [Cuzzi *et al.* 1993]), and laminar flow at later times.

Specifically, as a starting condition we choose a simple model where the gas density follows a simple $1/r$ dependence inside of $20R_J$ and outside of $26R_J$. The transition region

has a width of about $\sim 2H_c$, where H_c is the subnebula scale-height at the centrifugal radius of the primary. This choice ensures that the gradient in gas density is not so steep as to lead to a Rayleigh-Taylor instability (e.g., Lin and Papaloizou 1993). Our density profile is given by

$$\Sigma(r) = \begin{cases} \Sigma^0_{in}(R_{in}/r), & r < r_1; \\ a_1 r^{-b_1}, & r_1 < r < r_2; \\ \Sigma^0_{out}(R_{out}/r), & r > r_2. \end{cases} \quad (3)$$

where the relevant parameters for our various model choices are presented in **Table II**.

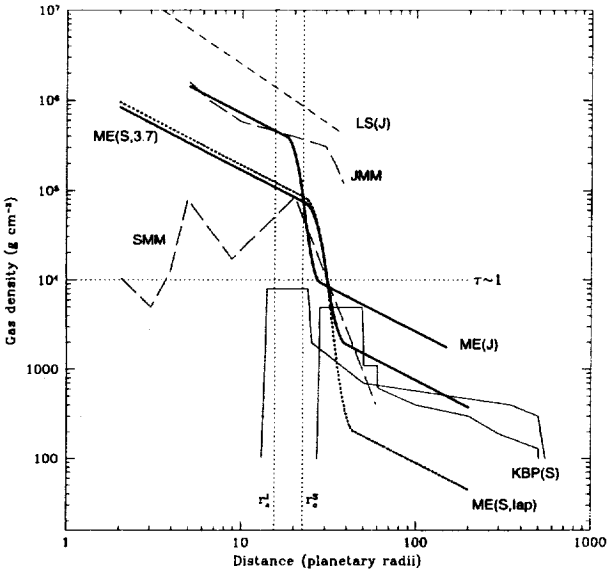

Figure 2: Comparison of gas surface density for our models as well as previous models for the Saturnian and Jovian systems. LS(J): Lunine and Stevenson (1982). JMM/SMM: The minimum mass model for Jupiter and Saturn respectively of Pollack *etal*▷ 1994. KBP: Spin out models of Korycansky *etal*▷ 1991 for Saturn. ME(J): Our minimum mass density profile for Jupiter after re-constitution of volatiles for Io and Europa. Disk size extends to $\sim 150R_J$. ME(S): Solid line indicates our model for Saturn in which the mass of solids in the subnebula is taken to be 3.7 times less that of Jupiter. Dotted line indicates our model in which the minimum amount of mass is placed outside of the orbit of Iapetus to form it. The location of both Jupiter's and Saturn's centrifugal radii are labeled.

In **Figure 2**, we plot the surface density as a function of radial location for our model for Jupiter and Saturn as well as other models in the literature. Though our model bears a close relation to the minimum mass model it differs in the distribution of mass in that we allow for an extended low density component. For Jupiter, the mass of Callisto is distributed in the outer disk. For Saturn, we do not spread the mass of Titan out to Iapetus as is done in the SMM model. Rather, we expect that most of the mass of Titan came from the inner disk which extends roughly out to the position of Hyperion. It should be noted that in our model the size of the inner disk of Saturn and Jupiter scale with the size of the planet's Hill radius, which leads to a more extended inner disk for Saturn. The surface density of Saturn's disk is smaller both because there is less mass in the satellite system and also because the mass is more spread out. We have plotted two curves for our Saturn model which differ mostly in the treatment of the outer disk. The solid curve corresponds to a model where we keep a constant mass ratio of 3.7 for the masses of the outer and inner disks of Jupiter with respect to the outer and inner disks of Saturn. The dotted curve was determined by the amount of material needed to make Iapetus out of the condensables present in the outer disk assuming a cosmic mixture (see Section 6). The curves labeled KBP correspond to cases for Saturn and should be compared to our Saturn curves. Notice the presence of an extended component out to $R_{roche}/2 \sim 500R_S$ for the KBP model. These correspond to the spin out scenario of Korycansky *et al.* (1991). The curves labeled LS(J) correspond to the work of Lunine and Stevenson (1982), which extended an adiabat from the planet to form a subnebula with several times more mass in solids than is present in Jupiter's satellite system.

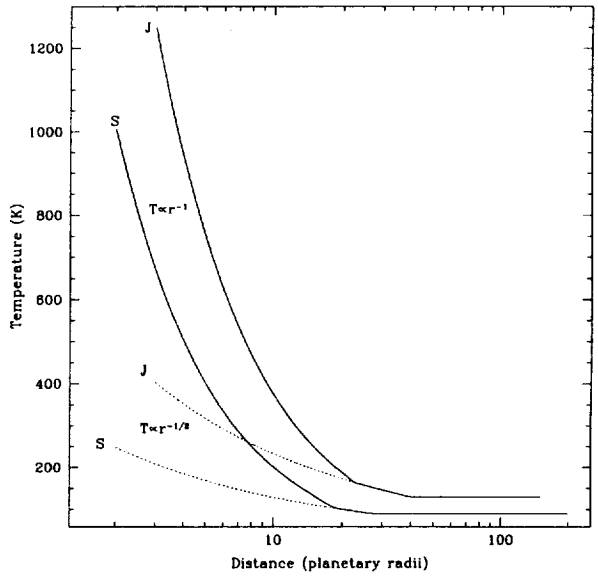

Figure 3: Temperature profiles used in our modeling. Inner disk temperature varies like r^{-1}. Transition in behavior to $r^{-1/2}$ occurs around the centrifugal radius of both planets. Temperatures at greater distances in the outer disk are isothermal. The temperatures in the outer disk are taken to be that of the equilibrium solar nebula temperature ($T_e \approx 280\sqrt{1AU/r}$) which is roughly 130 K for Jupiter and 90 K for Saturn. 250 K is set to coincide with the position of Ganymede for Jupiter, and Rhea for Saturn.

In **Figure 3**, we plot the temperature profile of the disks

of Jupiter and Saturn as a function of radial location. As one would expect, Saturn' disk has less variation in temperature. It bears remembering that this is the mean temperature distribution immediately following planetary accretion. Jupiter's cooling timescale is $\sim 10^7$ years and Saturn's is $\sim 10^6$ years (Pollack *et al.* 1976). Saturn's temperature profile will be described more fully in Section 6.

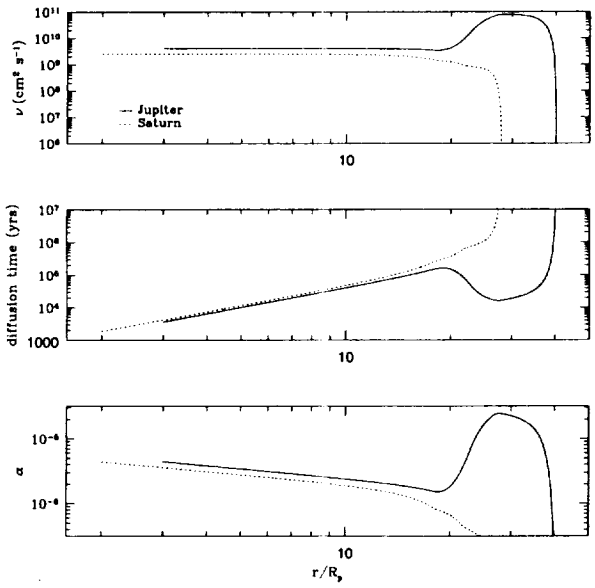

Figure 4: A plot of viscosity, diffusion time, and turbulence coefficient for Jupiter and Saturn's inner disk using our temperature profiles (see Figure 2). Low viscosities correspond to weak turbulence and long evolution times. The bumps present in the Jupiter curve but not the Saturn curve is due to the difference in the temperature profiles in the transition region.

For our optically thick disk where the temperature profile is determined by viscous dissipation we have

$$\Sigma\nu r^2 \left(\frac{d\Omega}{dr}\right)^2 = 2\sigma_{SB}\left(T^4 - T_0^4\right), \qquad (4)$$

where σ_{SB} is the Stefan-Boltzmann constant, T is the photospheric temperature, and T_0 is the nebula background temperature. In **Figure 4** we use the density profile of Figure 2, the temperature profile of Figure 3, the above equation, and the equation $t \sim r^2/\nu$ to plot the viscosity, the diffusion time, and the turbulence coefficient $\alpha = \nu\Omega/c^2$, where c is the speed of sound, as a function of position in the disk for Jupiter and Saturn (the Iapetus model was used for Saturn, see Section 6). It is clear that our temperature profile corresponds to the case of weak turbulence, with long evolution times. A viscosity bump is seen in the Jupiter curve but not the Saturn curve due to the difference in the temperature profiles in the transition region. In the case of Jupiter, this transition is significantly hotter than the background temperature (see Figure 3). Hence, the sharp drop in density leads to larger viscosity values as given by Eq. (4). On the other hand, Saturn's transition region has a temperature essentially equal to the background temperature, and so no viscosity bump is observed. Because the temperature profiles are set by assuming accretion temperatures for Ganymede and Titan, and are subject to significant modeling uncertainty, it is presently unclear how significant this viscosity bump is, or its effect on satellite accretion. It is interesting to note that the diffusion time of the inner disk increases with distance. As a result, the inner disk density profile (see Figure 2) will tend to flatten with time. Though some turbulence models may allow for the possibility of surface density profiles that increase with distance (Bell *et al.* 1997), more work will have to be done before it is understood whether that is a realistic possibility in the present context.

It is important to point out that our nebula is not vertically isothermal. The temperatures at the midplane are significantly larger than the photospheric temperatures. Hence, it is unlikely that satellite accretion can be thought of as a heterogeneous process with the rock component accreting at the same time as the ice component. Nevertheless, the ice/rock ratio of the large satellites indicates that this complication does not prevent accretion of either component. To the extent that non-homogeneous accretion can affect the final structure of the satellites, it will do so in the inner disk, where the cooling times are significantly longer and the accretion times shorter. Though our chosen temperature profile indicates that the satellite itself is in a hotter region of the disk, this may not pose a problem. Since the dynamical time is likely to be considerably faster than the timescale at which particles of size $\sim$ 50 m (the size at which particles decouple from the thick Jovian gas disk) melt and/or vaporize, a satellite at the Jovian midplane may still accrete water.

4 Galilean Satellite Accretion and Evolution

In analogy to gas-free planetary accretion we begin the problem of satellite accretion by calculating characteristic sizes of satellitesimals and satellite embryos for our disk parameters assuming a satellitesimal density of $\rho_s = 1.5$ g cm^{-3}. Though our problem differs markedly from one in which the satellites are accreted in the absence of gas, we will show later that the characteristic sizes one obtains in the presence of gas are roughly consistent with the ones we give below, which are meant only as a loose indication of typical object sizes. The characteristic length scale and mass scales over which the disk's self-gravity dominates shear is approximately $l_1 = r_H$, where $l_1 = (m_1/\pi\Sigma_s)^{1/2}$ and $r_H = a(m_1/3M_J)^{1/3}$ is the Hill radius of a satellitesimal of mass m_1 (*e.g.* Ward 1996). Using a surface density of solids of $\Sigma_s \sim 5 \times 10^3$ g cm^{-2} for the inner disk of radius $\sim 15R_J$, we obtain $m_1 \sim 1.6 \times 10^{17}$ g, which corresponds to a satellitesimal radius of $\sim$ 3 km and $l_1 \sim$ 32 km. The second characteristic mass and radial scale, $l_2 = m_2/(4\pi a\Sigma_s)$, is the distance over which Keplerian shear can force close encounters among satellitesimals $l_2 = r_H$. This gives $m_2 = 8\pi\Sigma_s a^2(\mu_d/3)^{1/2}$,

where $\mu_d = \pi\Sigma_s a^2/M_J$. Using the same surface density as before, we get $m_2 \sim 7.6 \times 10^{24}$ g, which corresponds to an embryo radius of ~ 1100 km and $l_2 \sim 1.2 \times 10^4$ km.

Assuming satellite formation is controlled by binary accretion of satellitesimals we can write the timescale for accretion as (Safronov 1969; Lissauer and Stewart 1993; Ward 1993)

$$\tau_{acc} \sim \frac{\rho_s r_s}{\Sigma_s \Omega} F_g^{-1}, \tag{5}$$

where F_g is the gravitational focusing factor. In the context of planetary accretion this focusing factor can be quite large during runaway growth. For satellites, however, the Hill radius r_H is never much larger than the physical radius r_s. An upper limit to the enhancement factor can be obtained (e.g., Weidenschilling, 1974) $F_g \sim (r_H/r_s)^{3/2} \sim O(10)$ for Ganymede. Then we can use Eq. (5) to obtain

$$\tau_{acc} \sim 4.8 \left(\frac{\rho_s}{1\,g\,cm^{-3}}\right)\left(\frac{r_s}{100\,km}\right) \times \left(\frac{10^4\,g\,cm^{-2}}{\Sigma_s}\right)\left(\frac{a}{20R_J}\right)^{3/2} F_g^{-1}\ years. \tag{6}$$

Given surface density of solids of $\Sigma_s \sim 10^3$ g cm^{-2}, this formula predicts a timescale of formation of ~ 100 years for a Galilean-sized satellite. This, however, assumes that all the solids in the disk at any one time are in the form of satellitesimals. Let us assume for the sake of discussion that at some time early on all the solids in the inner disk are in satellitesimals of characteristic size ~ 1 km. In that case, the time for drag to completely clear the inner disk of solids (see Eq. 9) would be a few years! Therefore, it is unlikely that the binary accretion timescale controls the process of satellite formation unless most of the mass resides in large satellitesimals. In the inner disk we expect turbulence (albeit weak) to be present during satellite accretion. Hence it may not be a valid assumption to start with a disk of satellitesimals. Instead we form satellites first by the sweep up of dust and rubble, followed by the accretion of inwardly migrating satellitesimals once a significant fraction of the solids in the disk have aggregated to satellitesimal sized objects.

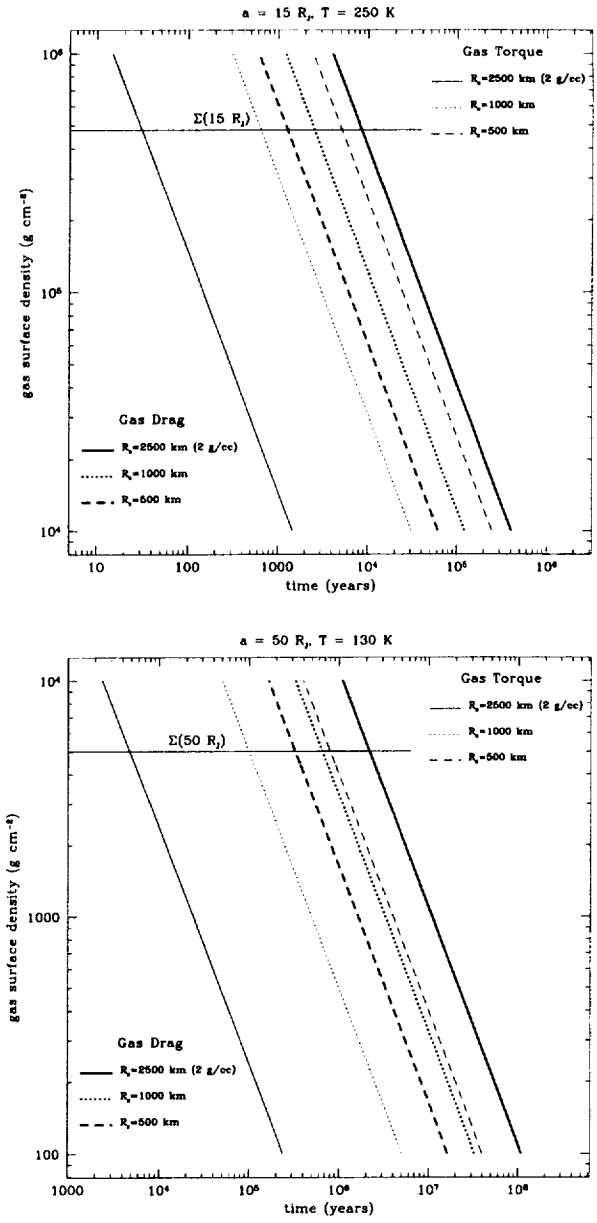

Figure 5: (a) Orbital decay times of satellitesimals of various sizes due to gas drag and gas tidal torque at $15R_J$. The gas surface density for our models is indicated in the plot for this radial location. The decay times of smaller objects is dominated by gas drag, while larger objects are controlled by gas tidal torque with the transition between 500-1000 km. (b) Orbital decay times of satellitesimals of various sizes due to gas drag and gas tidal torque at $50R_J$.

In **Figure 5**, we calculate the orbital decay timescales due to gas drag and tidal torque of a proto-satellite at $15R_J$ (a) and $50R_J$ (b) for a range of gas densities. Because the gas is partly supported by gas pressure, its orbital velocity v_{gas} is slightly lowered with respect to the Keplerian circular velocity v_K. An

object orbiting at Keplerian speed will therefore experience head-wind and drag towards the primary. A measure of the difference between the Keplerian velocity and the drag velocity is given by

$$\eta = \frac{v_K - v_{gas}}{v_K} \approx -\frac{r}{2\rho_g v_K^2}\frac{\partial P}{\partial r} \sim \left(\frac{c}{v_K}\right)^2, \quad (7)$$

where P is the gas pressure, and c is the speed of sound. The timescale for orbital decay due to gas drag is given by

$$\tau_{gas} = \frac{4\rho_s r_p v_K}{3C_D(\Delta v)^2}\frac{2c}{\Omega\Sigma} \quad (8)$$

where ρ_s and r_p are the satellitesimal density and radius, $C_D = 0.44$ is the Stokes flow regime drag coefficient for high Reynolds number, Ω is the orbital frequency, Σ is the gas surface density, and $\Delta v = \eta v_K$. The stopping time t_s can be written in terms of the timescale for radial migration $t_s = 2\Delta v \tau_{gas}/v_K$ (Weidenschilling 1988). We can write Eq. 8 in the form

$$\tau_{gas} \approx 22\left(\frac{\rho_s}{1\,g\,cm^{-3}}\right)\left(\frac{r_p}{1\,km}\right)\left(\frac{130\,K}{T}\right)^{3/2} \times \left(\frac{10^5\,g\,cm^{-2}}{\Sigma}\right) years. \quad (9)$$

The torque timescales are calculated using the formulation of Ward (1997). A generalized version of the torque exerted on the disk in the vicinity of an mth order Lindblad resonance (Goldreich and Tremaine 1978,1979; Ward 1997) is given by

$$T_m = -\pi m \Sigma \Psi_m^2 \left(r\frac{dD_*}{dr}\right)^{-1} \quad (10)$$

where Ψ_m is the forcing function of the satellite, and D_* is a function of the difference in local epicyclic frequency of the disk and the Doppler shifted forcing frequency, as well as the gas sound speed. A estimate of the forcing function that works well in cases far from the transition region is $\Psi_m \sim (2m-1)GM_s/a$, where M_s is the satellite mass and a is its position, with $m \sim a/H$, the resonance where most of the torque is deposited (Takeuchi *et al.* 1996), and $rdD_*/dr \sim 3\Omega^2$. We can write the orbital decay timescale due to tidal torque in terms of our subnebula parameters

$$\tau_{torq} \approx 3.2 \times 10^4\left(\frac{1\,g\,cm^{-3}}{\rho_s}\right)\left(\frac{100\,km}{r_p}\right)^3 \times \left(\frac{T}{130\,K}\right)^{3/2}\left(\frac{10^5\,g\,cm^{-2}}{\Sigma}\right)\left(\frac{a}{R_J}\right) years. \quad (11)$$

Using Equations (9) and (11) we can get a rough estimate of the transition size r_T of a satellitesimal where gas drag and gas torque are equivalent

$$r_T \sim 200\left(\frac{1\,g\,cm^{-3}}{\rho_s}\right)^{1/2}\left(\frac{T}{130\,K}\right)^{3/4}\left(\frac{a}{R_J}\right)^{1/4} km \quad (12)$$

which yields a size of ~ 500 km for a satellitesimal with density $\rho_s = 1.5$ g cm^{-3} at $15R_J$. For larger sizes, the gas torque dominates the satellite's evolution. Since the estimate given by Eq. (11) does not take into account that the net torque must be weighted by a measure of the torque asymmetry between inner and outer torques, this expression overestimates the strength of the net torque. Actual torque values used to produce the figures are calculated by summing over inner and outer resonances out to a value of $m >> a\Omega/c$. Such a torque produces mostly inwardly migrating satellites (Ward 1997; see Paper II for a more detailed discussion of the torque).

Figure 5 considers the evolution of satellites with $r_s =$ 500, 1000, and 2500 km as a result of gas drag and tidal torque separately. In Figure 5a, we show the orbital decay timescale for an object located at $15R_J$ for a range of gas densities appropriate to the inner disk ($\Sigma = 10^4 - 10^6$ g cm^{-2}). The decay times due to gas drag are typically shorter than those due to torque, however for the larger objects, the torque begins to dominate their evolution. In the inner disk the transition takes place for objects of size $\sim$ 1000 km. Similarly in Figure 5b, we show the orbital decay of an object starting at $50R_J$ where the gas density is much lower ($\Sigma = 10 - 1000$ g cm^{-2}). From this figure, it is clear that survival of a satellite in a gaseous medium (where most of the mass and angular momentum resides in the gas component) is an issue that needs to be addressed for objects of all sizes. Lengthening the satellite formation timescale in order to accommodate a partially differentiated Callisto makes this issue even more of a concern (see Section 5). So long as solar mixtures are used, decreasing the gas density is unlikely to help survival since that also decreases the surface density of disk condensables Σ_s. Thus, the ratio of the growth timescale by rubble and dust sweep up to the orbital decay timescale by gas drag remains the same (see discussion following Eq. 14). On the other hand, enhancing the concentration of condensables does improve the chances of satellite survival.

Given the short orbital decay times, we need to ask whether any solids present in the subnebula would survive long enough to make satellites. We argue here that the timescale for Galilean satellite formation is $\sim 10^3$ years, sufficiently short to survive inward migration. What happened after the satellite grew to its full size is discussed in Paper II.

We start by assuming the formation of satellitesimals as a result of particle aggregation (Weidenschilling and Cuzzi 1993). Though a gravitational instability (Goldreich and Ward 1973) probably did not take place (Cuzzi *et al.* 1993) it is still possible that other instabilities did (Goodman and Pindor 2000). Once satellitesimals form they quickly settle down to

the subnebula midplane. These objects continue to grow by dust and rubble sweep up or by accretion of other satellitesimals. Let's first consider the growth timescale due to dust and rubble sweep-up. Assuming that the particle sizes are small enough that they are entrained in the gas we can write the time scale as

$$\tau_{sweep} = \frac{4\rho_s r_p}{3\bar{\rho}_p \Delta v_p} \tag{13}$$

We can also write this equation in the form

$$\tau_{sweep} \approx 0.58 \left(\frac{\rho_s}{1\,g\,cm^{-3}}\right)\left(\frac{r_p}{1\,km}\right)\left(\frac{a}{R_J}\right) \times \left(\frac{130\,K}{T}\right)^{1/2}\left(\frac{10^5\,g\,cm^{-2}}{\Sigma}\right)\left(\frac{H_p}{H}\right) years, \tag{14}$$

where H_p is the particle scale height, H is the subnebula scale-height, and we have assumed a two-population particle size distribution where large particles move at essentially Keplerian speeds while the small particles are entrained in the gas. We have also assumed that the dust density is less than the gas density, and so the head-wind is not lowered by the dust concentration. That is, we let $\Delta v_p \approx \Delta v \approx \eta v_K$. Allowing for $H_p < H$, the sweep up timescale is smaller than the drag timescale for $a < 38R_J$; that far from the planet our model is optically thin, isothermal and quiescent. As a result, in the outer disk we expect $H_p << H$ (see Section 5). In the inner disk we expect $H_p < H$ during most or all of the satellite accretion process. Quite generally, then, this model yields shorter sweep up times than drag times, thus favoring the formation of satellites. In the inner disk (inside of $15R_J$, $T = 250$ K), where the temperature is inversely proportional to the radial location, the ratio of the sweep up time to the gas drag time is independent of semi-major axis and particle size $\tau_{sweep}/\tau_{gas} \sim H_p/H < 1$. This result makes it possible to form satellites of any size < 1000 km (such that gas drag dominates their inward migration) at any radial location in the inner disk.

In the presence of turbulence, balance is established between the rate of diffusion of dust due to turbulence and the rate of settling due to gravity. The scale height of dust is then given by

$$H_p \approx \left(\frac{\nu}{Sc}\frac{C_H}{\Omega^2 t_s}\right)^{1/2}. \tag{15}$$

where the Schmidt number is approximately given by $Sc = 1 + \Omega t_s$, and $C_H \approx 1$ is a constant. We expect accretion to take place under weak turbulence ($\alpha \sim 10^{-6} - 10^{-5}$) which corresponds to turbulent viscosity $\nu \sim 10^{10}$ cm^2 s^{-1} (see Figure 4). For 1 cm particles we get $H_p \sim 0.2H$. Then the sweep-up timescale for a 1000 km object becomes $\tau_{sweep} \sim 10^3(H_p/H) \sim 200$ years. Notice also that dust of size 1 cm will diffuse a distance $d \sim (t\nu/Sc)^{1/2} \sim 0.1R_J$ in a time $t = 2\pi a/\Delta v$ due to gas turbulence. Since this is much larger than ~ 1000 km, the embryo will not clear its lane.

This timescale is likely to overestimate the time it would take to form such a satellite embryo for three reasons. First, dust will coagulate and settle to the midplane, thus lowering the sweep up time (as it settles it will migrate and grow). Second, the turbulence itself may die down further for optically thin disks (though the timescale for this to happen may be longer than the satellite accretion timescale). Third, an embryo will also grow due to capture of inwardly migrating satellitesimals. The process of dust coagulation is complicated, and we will not address it at this time.

Thus, satellite embryos can be made sufficiently quickly to survive inward migration due to gas drag. It is important to notice that sweep-up and gas drag are both proportional to the object's radius. As a result, sweep up growth is sufficiently fast for embryos of all sizes to survive. On the other hand, it is possible that global turbulence persists long enough for some satellite embryos to be lost due to inward migration. At any rate, inward migration of satellite embryos appears very likely. This would not be a serious problem since most of the mass would then still be contained in the puffed-up dust and rubble disk. The issue becomes how to prevent mass loss in growing embryo-sized objects to satellite-sized objects.

As we noted before, for objects larger than 1000 km, migration due to gas torque becomes dominant over migration due to gas drag. Since the orbital decay time due to torque of a Galilean-sized object is again about 10^3 years, one might be tempted to simply continue sweeping up dust and rubble. However, so far we have assumed a large reservoir of dust and rubble such that the surface density to be swept did not change as the embryo grew. Clearly, as the surface density of dust and rubble decreases so will the efficiency of this process. In any event, coagulation of dust and possibly the decay of gas turbulence make it likely that embryos grew to satellite size by accretion of satellitesimals.

We first define the feeding zone of a satellite embryo. During closest approach, a satellite embryo will pump the eccentricity of a previously circular satellitesimal by the amount $e = 2.24(m_s/M_J)(a/s_l)^2$ (Julian and Toomre 1966), where m_s is the mass of the embryo and s_l is the separation between the two objects. Crossing orbits will result if $s_l = ae$. Using this condition we obtain $s_l = a(2.24m_s/M_J)^{1/3}$ for the size of the embryo's feeding zone. (*i.e.* we take the feeding zone to be $\sim 2r_H$; this is slightly more conservative than the value for the feeding zone $2\sqrt{3}r_H$ one obtains using Jacobi's constant and asking that the separation between the two bodies be such that they never experience close approaches). One can now define an embryo size such that most satellitesimals dragging into its feeding zone will be accreted. Suppose we take a satellitesimal of mass m_1, which corresponds to a radius ~ 3 km. Such a satellitesimal has a very fast evolution timescale of ~ 8 years. We calculate the drag distance $l_d = (v_d 2\pi a/3\Omega)^{1/2}$ (with $v_d = a/\tau_{gas}$) such that $2l_d$ is the distance a satellitesimal will drag after one synodic period of two objects a distance l_d

from each other. Then using the condition $s_l = l_d$ we calculate an embryo mass $m_d \sim 2.2 \times 10^{25}$ g, which corresponds to an object size $\sim$ 1500 km, and a feeding size of $s_l \sim 32000$ km. The time it took for the satellitesimal to cross this feeding zone (assuming that satellitesimal growth can be ignored; *i.e.* the embryo has cleared its feeding zone) was $\sim$ 0.22 years (the synodic time of two objects separated by $\sim$ 32000 km at $15R_J$). If we increase the concentration of solids by a factor of 4 then the embryo size becomes 760 km (the smaller embryo size results from the longer satellitesimal orbital decay times in a disk with 4 times less gas). Hence once an embryo has reached a size $\sim$ 1000 km its growth rate is controlled by the inward drift time of the characteristic size of the satellitesimals it accretes. If it mostly accretes kilometer sized satellitesimals the time between the embryo stage to full satellite is tens of years. On the other end, if most of its mass comes from the accretion of other embryos then the upper limit on the satellite accretion timescale is 10^4 years.

There are two mechanisms that limit the efficiency of drift augmented accretion. First, resonant capture may prevent satellitesimals from reaching the embryo. This, however, may not be an issue for the inner disk (or for the outer disk, though for a different reason; see Section 5). The embryo is not massive enough to prevent the orbital decay of kilometer sized objects given the gas surface densities of the inner disk (but see Section 6.2 where we discuss the resonant capture of Hyperion by proto-Titan, and the absence of a corresponding object for Ganymede). Second, the drifting satellitesimal may "horseshoe" around the embryo and avoid being captured by it. Kary *et al.* (1993) give impact probabilities for various mass ratios of the secondary to the primary as a function of the secondary's physical radius divided by its Hill radius. For a 1500 km embryo with density $\rho_s = 1.5$ g cm^{-3} this ratio is $r_s/r_H \sim 0.1$. As the embryo grows to satellite size the ratio will decrease slightly (due to the slight increase in its density). On the other hand, its feeding zone will increase and it will get more chances to capture any given satellitesimal. Hence we expect that the capture efficiency will improve slightly as the embryo grows (though for sufficiently large embryo masses, such that the gas flow around the secondary is changed significantly or a gap is opened, the efficiency may again decrease). Given the criterion used to calculate the embryo size, we are in the gas regime of significant impact probability. Then from Kary *et al.* (1993) (their Figure 9) we see that the impact probability for the case such that $r_s/r_H = 0.1$ is between 0.6 and 0.85 (in the limit that gas drag effectively damps eccentricities and inclinations of the feeder population). This impact probability is high enough that a minimum subnebula model may apply to the accretion of satellites (by contrast, giant planet cores have much smaller ratios of the physical size to their Hill radius, and are therefore unable to efficiently capture inwardly drifting planetesimals). This is a significant result. It says that $\sim$ 1000 km satellite embryos are effective barriers, and will capture most inwardly migrating satellitesimals, thus limiting the amount of material that is allowed to spiral into the planet or inner embryos.

As we will see in Paper II, we expect that satellites of a sufficient size produce a feedback reaction on the gas disk which stalls their inward migration. An even larger satellite may open a gap in the subnebula. While satellite embryos may have migrated as they grew to a size of 1000 km, once they reached this size continued growth might have been fast enough to avoid further inwards migration. The locations of Ganymede and Titan, just inside the centrifugal radii for Jupiter and Saturn, tend to make us think that these two satellites grew sufficiently fast to avoid significant inward migration (because of its slower accretion, Titan may have migrated more than Ganymede despite Saturn's lower gas density). In general though, satellites are likely to have drifted significantly before the feedback reaction of the torque was large enough to stall their inwards migration. In Paper II we use this to explain the mass to distance relation of the Saturnian and Uranian satellite systems.

In order to obtain an embryo size that becomes an effective barrier for inwardly drifting satellitesimals a typical satellitesimal mass m_1 was used. We now attempt to provide further justification for this choice. As we mentioned before, one expects the dust and rubble scale-height eventually to decrease due to the effects of coagulation and turbulence decay. We consider a case such that the coagulation of dust produces particles that decouple from the gas in a timescale shorter than 10^3 years. First we find the characteristic particle size that will decouple from the gas. Given our nebula parameters and using the condition $\Omega t_s \sim 1$, we obtain a particle size $\sim$ 50 m in the region between $15 - 20R_J$. This particle settles to the midplane and drifts in due to gas drag. As it does, it grows by sweep up of smaller particles. Assuming a self-similar power law distribution as in Weidenschilling (1997), we use particles of size $\sim$ 10 m as the feeder population where most of the mass resides. We calculate the scale-height for these particles under strongly turbulent conditions ($\alpha \sim 10^{-4} - 10^{-3}$) using equation (13) and obtain $H_p \sim 0.04H$ (head-wind decreases for $H_p < 0.01H$ such that the particle layer density $\bar{\rho}_p > \rho_g$). For weak turbulence ($\alpha = 10^{-6} - 10^{-5}$) the scale-height for the same feeder particle would be an order of magnitude smaller.

We can now calculate the time it takes for a 50 m particle at $20R_J$ to evolve to $15R_J$ and the size it will grow to by the time it gets there. The size of the satellitesimal is given by solving

$$\frac{dr_p}{dt} = \frac{\Sigma_s c}{8\rho_s \beta a} = \frac{g_1(a,t)}{a}, \qquad (16)$$

where $\beta = H_p/H$, and the initial size of the satellitesimals is taken to be the size of the object such that $\Omega t_s \sim 1$. The drift velocity of this satellitesimal is

$$v_d = \frac{da}{dt} = -\frac{3C_D \Sigma c^3}{8\rho_s G M_P} \frac{a}{r_p} = \frac{g_2(a,t)}{r_p}, \qquad (17)$$

We can decouple these equations by letting $r_p = g_2/(da/dt)$ and plugging this into (16). For the inner disk, the temperature

varies like $1/r$ (which implies $g_1, g_2 \propto a^{-3/2}$) so that the position of the satellitesimal as a function of time is given by

$$\frac{d^2a}{dt^2} = \frac{1}{a}\left[\frac{a^2}{75C_D\beta H^2} - \frac{3}{2}\right]\left(\frac{da}{dt}\right)^2 = \frac{1}{a}\Lambda\left(\frac{da}{dt}\right)^2, \tag{18}$$

Assuming that β is constant then Λ is constant and we can solve this equation exactly to give the particle velocity as a function of time

$$v(t) = v_0\left[1 + (\Lambda - 1)\frac{|v_0|}{a_0}t\right]^{-\frac{\Lambda}{\Lambda-1}} \tag{19}$$

where v_0 is the initial velocity of a satellitesimal of initial size r_{p0}. We can now integrate this equation for our subnebula model to give an equation for time as a function of position

$$t_G = \frac{a_0}{|v_0|(\Lambda - 1)}\left[\left(\frac{a_0}{a}\right)^{\Lambda-1} - 1\right] \tag{20}$$

and finally the growth of the satellitesimal as a function of time

$$r_p(t) = r_{p0}\left[1 + (\Lambda - 1)\frac{|v_0|}{a_0}t\right]^{\frac{\Lambda+3/2}{\Lambda-1}}. \tag{21}$$

We find that for the case of strong turbulence a 50 m particle will take $t_G \sim 0.2$ years to drift between $20R_J$ and $15R_J$ and it will grow to a size of ~ 1 km, which may be a bit small to be efficiently accreted by an embryo. However, for the case of weak turbulence, growth occurs much more quickly. In this case, the same particle grows to a size of ~ 10 km in ~ 0.2 years after $\sim 1R_J$ of inward migration. Once satellitesimals have attained this size they are likely to get picked up by embryos inside of their own orbit. While this model is quite sensitive to the particle sizes chosen, it does point out that particles that decouple from the gas and drift in are subject to growth. This growth may be fast enough that most of these particles will become satellitesimals with sizes > 1 km after only a few R_J of inward migration, at which point they will slow down and eventually get captured by a satellite embryo inside their own orbit. Although uncertain, this calculation is roughly consistent with the gas-free calculation of characteristic satellitesimal sizes. This again points out that the minimum mass model may indeed provide a fair estimate of the mass of condensables initially present in the gas disk.

Several workers have pointed out that Safronov style accretion has difficulties explaining the masses of the Galilean satellites (Coradini *et al* 1981; Richardson *et al.* 2000), but these studies do not take into account the effects of gas drag. We have shown that gas drag will play a major role in shaping the properties of the Galilean satellites. First, gas drag might deplete inner portions of the disk (the extreme case of which might be Saturn's system which has little mass inside of Titan). Second, the scenario discussed above leads one to the view that satellites grew by accreting material outside of their own orbit delivered to them by gas drag. Such a model can be used to explain not just why Io and Europa are water deprived, but also why Europa would turn out smaller than Io. Since the feeding zones of the satellites grow with distance as their Hill radius increases and Europa accreted some water one might expect the reverse to be the case. In our model the growth of a satellite depends on the growth of its outer neighbor. As a result, one would expect a large satellite to be preceded by a small one. That is, we believe Ganymede probably prevented Europa from growing to Io size. In such a model it may not be surprising to find that the object with the most mass accretes close to the centrifugal radius (note that this is also true for Saturn's satellite system). Outside this radius the gas density decrease may lead to smaller satellites. Inside of this radius the growth of the satellite may be limited by the growth of its outer neighbor.

5 Slow Formation of Callisto

Our model has Callisto forming from an extended, low optical depth gas disk. Since the disk will quickly become isothermal once grain coagulation leads to optical depth much less than unity, we expect this gas disk to be largely quiescent with very low gas viscosity. This means that the dust and rubble layer will quickly settle down to the midplane within a scale-height much smaller than the gas scale-height. The size of the dust and rubble layer is determined by local shear turbulence close to the midplane (Cuzzi *et al.* 1993).

First we calculate characteristic masses and lengths in analogy to the planetary accretion problem (*e.g.* Ward 1996) for the case in which the outer disk contains $\sim M_{Callisto}$ of solids. At $\sim 50R_J$ with $\Sigma_s \sim 53$ g cm^{-2} and $\rho_s = 1.5$ g cm^{-3}, we obtain $m_1 \sim 2.9 \times 10^{14}$ g, which corresponds to a satellitesimal radius of ~ 0.36 km and $l_1 \sim 13$ km. The embryo size is $m_2 \sim 3.3 \times 10^{23}$ g, which corresponds to a embryo radius of ~ 370 km and $l_2 \sim 1.4 \times 10^4$ km.

If we perform the same calculations further out at $\sim 100R_J$ with $\Sigma_s \sim 26$ g cm^{-2}, we obtain $m_1 \sim 2.3 \times 10^{15}$ g which corresponds to a satellitesimal radius of ~ 0.72 km and $l_1 \sim 53$ km. The embryo size is $m_2 \sim 9.2 \times 10^{23}$ g which corresponds to a embryo radius of ~ 530 km and $l_2 \sim 3.9 \times 10^4$ km. These characteristic masses are about an order of magnitude smaller than the masses we obtained at $15R_J$ for m_2 and two orders of magnitude smaller for m_1.

Given the low scale-height of the particle layer similar size embryos form quickly. Hence in this case it may not be a bad assumption to consider growth timescales in a case such that the solids in the disk are in the form of satellitesimals. For the outer disk the Safronov accretion time is given by:

$$\tau_{acc} \sim 10^5 \left(\frac{\rho_s}{1\,g\,cm^{-3}}\right)\left(\frac{r_s}{100\,km}\right)\left(\frac{10\,g\,cm^{-2}}{\Sigma_s}\right) \times \left(\frac{a}{150R_J}\right)^{3/2} F_g^{-1}\,years. \quad (22)$$

Using a density of solids in the outer disk $\Sigma_s \sim 10$ g cm^{-2} and enhancement factor $F_g \sim O(1)$, this formula predicts that an embryo with $\rho_s = 1.5$ g cm^{-3} and size ~ 500 km would be formed in $\sim 10^6$ years at $150R_J$. Several factors can alter this growth timescale. Larger values of the enhancement factor can speed up the growth of large objects in the outer disk. However, even though the Hill radius of an embryo is much larger than its physical radius, the low density of embryos leads to infrequent collisions and velocity dispersions comparable to the escape velocity of the embryos (see Appendix A). As a result, the focusing factor is unlikely to be much larger than one. On the other hand, embryo collisions do not necessarily lead to accretion. Glancing collisions may not lead to sticking or may yield embryo spins resulting in ejection. Furthermore, collisional disruption of embryos > 100 km can decrease the efficiency of the growth process (see Appendix B). Finally, the above estimate was obtained assuming that all of Callisto was spread out to $150R_J$. Placing a fraction of Callisto's mass would lead to longer embryo growth times. Placing a fraction of Callisto's mass in the outer disk would lead to longer embryo growth times, but then Callisto may differentiate. From this we conclude that embryos with sizes $\lesssim 500$ km may be formed in a timescale of $\sim 10^6$ years at $\sim 100R_J$.

To find the characteristic sizes of outer disk embryos in the presence of gas drag we turn to drift augmented accretion. In the absence of global turbulence, we make the assumption that local turbulence due to the gas-dust shear layer close to the subnebula midplane will adjust itself to maintain rough parity such that $\bar{\rho}_p \approx \rho_g$ (Cuzzi *et al.* 1993). This approximate relation can be used to estimate H_p. Alternatively, we can write

$$H_p = C_T \frac{\Delta v}{\Omega^2 t_s} \quad (23)$$

where $C_T \approx 0.01$ is a constant (Cuzzi *et al.* 1993). The scale height is $H_p \sim 0.01H$ for particle of size ~ 10 cm. As we did in the case of Ganymede, we now calculate the sweep up time for a particle with radius r_p. We find $\tau_{sweep} \sim 5.5(r_p/1\,km)$ years at $50R_J$ and $\tau_{sweep} \sim 22(r_p/1\,km)$ years at $100R_J$. These growth timescales are ~ 50 times faster than the drift times in the presence of gas drag and gas tidal torque for any given object size (see Figure 5b).

The above sweep up times do assume that the dust and rubble surface density stays constant. Once the sweep up growth slows down due to dust and rubble depletion, continued embryo growth will depend on the drift augmented accretion of satellitesimals. As we did for the inner disk, we now ask what size embryo stands a significant chance of capturing satellitesimals of characteristic size m_1 drifting into its feeding zone. We choose the criterion $s_l = l_d$ as we did before, and find the characteristic quantities $m_d \sim 2 \times 10^{24}$ g, which corresponds to an embryo size of 690 km (for $\rho_s = 1.5$ g cm^{-3}), and $s_l \sim 4.8 \times 10^4$ km at $50R_J$. At $100R_J$ we get $m_d \sim 1.2 \times 10^{24}$ g, corresponding to a radius of 580 km, and $s_l \sim 8 \times 10^4$ km. A wrinkle results from the small scale-height and long drag times inherent in this problem. If we calculate how long it took satellitesimal m_1 to cross a distance l_d we find $t_d \sim 3$ years at $50R_J$ and $t_d \sim 10$ years at $100R_J$. This timescale is sufficiently long to allow some satellitesimal growth during the time it takes to cross the embryo's feeding zone. Taking this effect into account the corrected embryo sizes turn out to be slightly smaller 590 km at $50R_J$ and 540 km at $100R_J$.

The first thing to notice is that the smaller embryo mass now corresponds to the larger semi-major axis. This is because the larger value for m_1 at $100R_J$ led to longer timescales to cross the feeding zone, thus requiring a smaller embryo size to satisfy our capture condition. Even though the smaller embryo size now occurs further out, the decrease in size is not sufficient to compensate for the decrease in gas surface density. The result is that inner embryos will drag in first and drift augmented growth will stop (the small scale-height means that all the dust and rubble will quickly become depleted). Thus in our model 500 km represents the characteristic size that form before drifting in to Callisto's radial location. It is important to point out that this characteristic size decreases significantly if one considers disks of higher solid concentration (higher solid concentration disks may be desirable for several reasons; see also Paper II). For instance, if we keep the surface density of solids constant but decrease the gas density by a factor of 4 we obtain $m_d \sim 1.4 \times 10^{23}$ g, which corresponds to a size of ~ 280 km at $100R_J$.

As before, we need to address the issue of the capture efficiency. For the outer disk, the gas density is too low and the mass of the satellitesimals too high to avoid being captured into resonances if initially placed in low eccentricity orbits. However, proto-Callisto may not have captured objects into resonance because the typical (for embryo sizes in the range $100 - 500$ km) embryo eccentricities near Callisto's orbital location are given by $e \sim 0.02 - 0.07$, where we have assumed that the random velocities are on the same order as their escape velocities (Appendix A). These eccentricities are similar or larger than the critical eccentricity for which capture probability sharply drops off $e_{crit} \sim \eta \sim 0.03$ (Malhotra 1993). Hence, for low gas surface densities typical satellitesimal eccentricities may again lead to low probability of resonance capture. We have already pointed out that in the inner disk the gas drag may be too strong for resonant capture of a satellitesimal by an embryo. It is possible this leaves the transition region as the only place where resonant capture probability is significant (see Section 6.2).

Having established that resonant capture is unlikely to take place, we ask what fraction of the population of objects that

drift into Callisto's feeding zone will be accreted by it. In the case of Callisto, the synodic timescale is much shorter than the drift time across the feeding zone of the population of feeders. In this weak gas regime, the accretion efficiency is limited by the inclinations of the drifting satellitesimals. Typical inclinations for such objects are smaller than their eccentricities (see Appendix A). In the neighborhood of Callisto $i_H = ia/H \sim 0.06 - 0.26$ (for embryos in the range $100 - 500$ km). Given that for Callisto $r_s/r_H = 0.048$, we can use the simulations in Kary *et al.* (1993) (their Figure 12) to estimate the accretion probability at $0.7 - 0.8$. Hence Callisto will capture most of the satellitesimals that drift into its feeding zone (this argument also applies to proto-Callisto nearly unchanged).

We can now calculate the time it takes to accrete Callisto by the time it takes gas drag to clear the outer disk of such embryos. Such a calculation yields an accretion timescale for Callisto of $10^5 - 10^6$ years. This is calculated under the conservative condition that the gas density in the outer disk does not decrease over time. Since we expect that the assumed concentration of solids in the disk is if anything somewhat lower than the actual concentration (see Paper II), which would lead to longer accretion timescales. For instance, a concentration factor of 4 would lead to embryo sizes $\sim$ 300 km, which would take 2×10^6 years to drift in from $150R_J$ to Callisto's radial location (this timescale was obtained by integrating Eq. [17] with $\rho_s = 1.5$ g cm^{-3}). We give $\sim 10^6$ years as the clearing time for the outer disk. Since this timescale is significantly shorter than the gas dissipation timescale (taken to be 10^7 years), no embryos would be stranded outside of Callisto.

The upshot is that Callisto's accretion timescale differs significantly from that of Ganymede because Callisto must draw materials from much further out $\sim 150R_J$ (compared to $23R_J$ for Ganymede). To complete its accretion it must contend with the drag times of embryos. Since the gas density is much lower in the outer disk, the distances larger, and the dynamical times longer, the resulting accretion timescale for Callisto accretion will be much longer ($\sim 10^6$ years) than it was for Ganymede ($\sim 10^3 - 10^4$ years). It also possible that particulate matter coupled to gas flowing through the gap after gap-opening lengthens Callisto's accretion timescale but not that of Ganymede. The reason for this is that once Jupiter accretes most of its mass the specific angular momentum of gas flowing into its Roche-lobe is high enough to take this gas into radial locations outside the centrifugal radius. Proper accounting of the angular momentum budget of this gas component needs to include the torque of the Sun on the gas flowing into Jupiter. Given that a satellite collects most of the material outside its own orbit, Callisto is more likely to derive solids from this component than Ganymede. However, since at these late times most of the mass is likely to be in the form of planetesimals (Weidenschilling 1997) it is unclear whether this component can contribute a significant fraction of Callisto's mass. Yet another possible difference between the two satellites is that while Callisto is likely to have accreted homogeneously the same may not be true for Ganymede. The reason for this is that in the case of Callisto the satellite formation time is considerably longer than the disk cooling time at its location, whereas for Ganymede the two timescales are comparable. This difference could have played a significant role in the final structure of the two satellites.

The question arises whether even a million year accretion timescale is slow enough for the heat that gets buried as a result of the impacts with such large objects to be removed in time to avoid deep melting and runaway differentiation. More work will need to be carried out to check into this possibility. Here we simply point out a few factors that need to be taken into consideration. First, our impacts take place at the escape velocity of proto-Callisto. Hence heat gets buried only at the late stages of the accretion process. Second, such impacts bury heat but also upturn the upper layers of the satellite, thus leading to faster cooling times. Third, greater solid concentrations would lead to longer accretion times and smaller impactor sizes (the value for m_d decreases with slower drift rates). An object 300-500 km in radius impacting at the escape velocity could produce a layer of water tens of kilometers in depth if all of the energy is placed into the melting process. However, this calculation does not constrain how deep such an impact would penetrate the surface. Conservative estimates based on computations and experiments give depths roughly the radius of the impactor in this energy regime (Melosh 1989), taking into account the material displaced as well as excavated. Excavation depths would most likely be a considerable factor less than this, perhaps $\sim r_s/3$ (Melosh 1989). Thus, even an object as large as 500 km may be consistent with recent findings concerning the depth of clean ice on Callisto (Anderson *et al.* 2001). Pending further work, we conclude that that our model may lead to the accretion of a partially differentiated Callisto.

Such an accretion model can also account for the preferential retention of ices more volatile than water in Callisto compared to Ganymede, and for the large angular momentum stored in Callisto, which is only a small fraction of the angular momentum that was initially present in the extended disk of solids out of which it was accreted. Furthermore, our accretion model makes Callisto in regions of the gas disk that are not connected with high-optical depth regions where the temperature and density might have led to the production of reduced ices such as methane and ammonia. As a result, we would expect that Callisto is made of solar nebula composition, which contains mostly oxidized ices (though methane is present in many solar system objects).

It is natural to ask how sensitive are these calculations to the size of the disk. It turns out that the characteristic size of the embryos does not change much with disk size. This is because of the countering effects of the increase in Hill radius with semi-major axis and the decrease in surface density. A smaller disk size would yield similar embryo sizes which would take a slightly shorter time to evolve to Callisto. A larger disk can also be considered, but in that case one would need to explain why the irregular satellites were not dragged into the planet.

6 Saturn's Regular Satellite System

In order to apply our model to Saturn we first need to constrain the nebula parameters for Saturn as we did for Jupiter. First, we note that the ratio of the reconstituted Galilean satellite masses to the Saturnian satellite masses is ≈ 3.7. On the other hand, the ratio of the atmospheric envelopes of Jupiter to Saturn is ≈ 3.7 for giant planet core masses of ≈ 12 Earth masses, consistent with nominal values.

The above arguments apply to the inner disk where most of the mass resides. We now attempt to estimate the amount of gas present in the outer disk of Saturn. It must be kept in mind that the history of Saturn might have been substantially different from that of Jupiter. Nevertheless, it is instructive to apply the same sort of gap opening argument to Saturn as we applied to Jupiter. Using the torque of Saturn on its feeding zone (Eq. [1]) and assuming $\Delta \sim 0.13 a_S > H_S$, where H_S is the thickness of the solar nebula at Saturn (which is marginally satisfied), we find $\tau^S_{gap} \approx 3.5 \tau^J_{gap}$. Then the total mass in the disk is given by $M^S_{disk} \sim M_S \tau^S_{gap}/\tau^S_{acc} \sim M^J_{disk} \tau^J_{acc}/\tau^S_{acc}$. The resulting disk mass ratio is likely to be substantially less than the 3.7 we are using for the inner disk. However, this calculation is substantially uncertain. For one, it is unclear if the concept of gap-opening applies to Saturn at all. As a result, we will use two models. The first model simply assumes the same mass ratio to the Jovian system. The second model puts just enough mass between $60R_S$ and $200R_S$ to make Iapetus (since Iapetus is made of ice the minimum mass model requires a subnebula of $\sim 200 M_{Iapetus}$). This is in rough agreement with a model that makes Saturn in 10^7 years. These two models are shown in Figure 2.

We get a disk size of $\sim 220R_S$ by scaling the outer disk of Jupiter ($\sim 150R_J$) by the ratio of the Hill radii of Saturn and Jupiter. It is encouraging to note that Phoebe is located at $215R_J$. This object has a retrograde orbit of high inclination and eccentricity, leaving little doubt that it was captured. Therefore, we adjust the size of Saturn's outer disk slightly to $\sim 200R_S$ to fit in with the location of Phoebe. As was the case with the irregular satellites of Jupiter, we use gas drag to explain the absence of captured objects inside the orbit of Phoebe (though a couple of small irregulars have been found just inside of Phoebe). This scenario fits well with the capture theory of Pollack *et al.* (1979), in which Phoebe was captured as it passed through the envelope of proto-Saturn, and was left stranded by the subsequent collapse of the envelope.

To constrain the temperature of the Saturnian subnebula we simply assume that the accretion of methane ice explains the methane in Titan's atmosphere (Lewis 1972). That sets a temperature of ≈ 100 K at $20R_S$. Inside this location the subnebula is taken to be optically thick and the temperature to vary inversely with radius. In Figure 3, we have plotted the subnebula temperature as a function of distance in units of the planetary radius. For times $\sim 10^6$ years after accretion, the planet has had a chance to cool and we simply assume a constant temperature everywhere equal to the solar nebula temperature at the location of Saturn ~ 90 K.

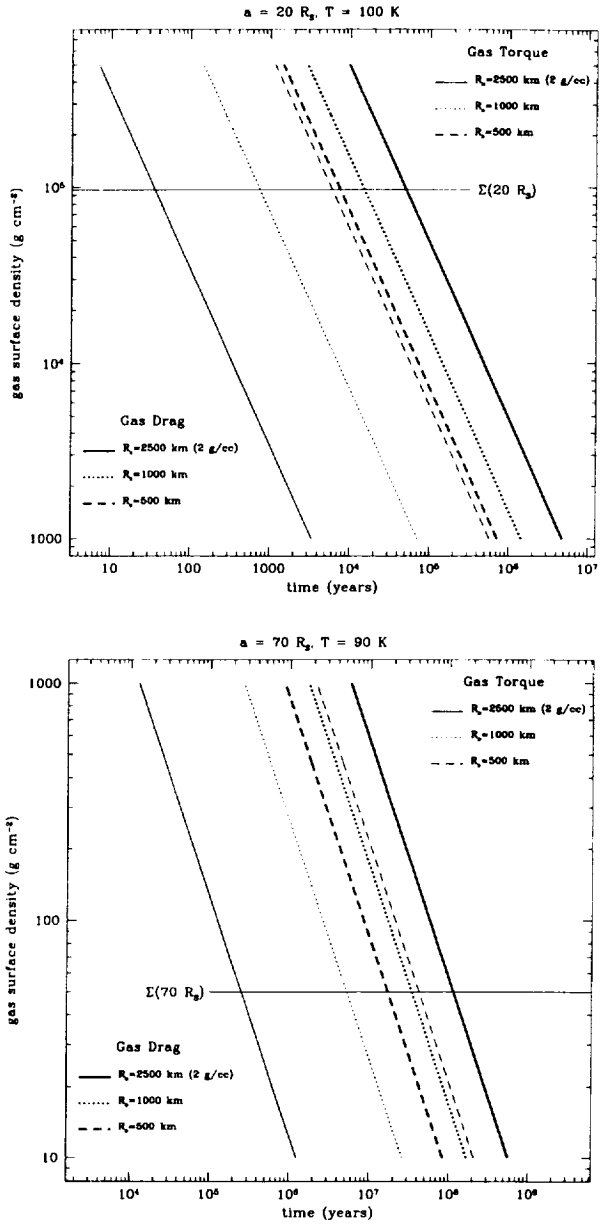

Figure 6a: (a) Orbital decay times of satellitesimals of various sizes due to gas drag and gas tidal torque at $20R_S$. The gas surface density for our models is indicated in the plot for this radial location. The decay times of smaller objects is dominated by gas drag, while larger objects are controlled by gas tidal torque with the transition between 500-1000 km. (b) Orbital decay times of satellitesimals of various sizes due to gas drag and gas tidal torque at $70R_J$.

As we did before in the case of Jupiter, we calculate characteristic masses based on the planetary accretion model. In Saturn's inner disk at $\sim 20R_S$ with $\Sigma_s \sim 900$ g cm^{-2} and $\rho_s = 1.5$ g cm^{-3}, we obtain $m_1 \sim 2.9 \times 10^{16}$ g which corresponds to a satellitesimal radius of ~ 1.7 km and $l_1 \sim 30$ km.

The embryo size is $m_2 \sim 1.8 \times 10^{24}$ g which corresponds to a embryo radius of ~ 660 km and $l_2 \sim 1.2 \times 10^4$ km.

In **Figure 6a**, we plot the orbital decay times at $20R_S$ as a function of the surface gas density for several particle sizes. As one would expect, even for the same surface density these evolution times are generally longer than those we calculated for the case of Ganymede. The reason for this is simply that the orbital period at Titan is longer than the orbital period at Ganymede. If we add to this the fact that the surface density of Saturn is lower than that of Jupiter (See Figure 2) because Saturn's disk is 3.7 times less massive and also more spread out (Saturn's Hill radius is larger), we end up with evolution times in Saturn's disk that are generally about an order of magnitude longer than the corresponding evolution times in Jupiter's disk. It is instructive to write the drag times at Saturn as

$$\tau_{gas} \approx 13 \left(\frac{\rho_s}{1\,g\,cm^{-3}}\right)\left(\frac{r_p}{1\,km}\right)\left(\frac{90\,K}{T}\right)^{3/2} \times \left(\frac{10^5\,g\,cm^{-2}}{\Sigma}\right) years. \quad (24)$$

Now we turn to the process of forming satellites by the same method as we used in the case of Jupiter. First we build up embryos using sweep up of dust and rubble. The timescale for this process at Saturn is

$$\tau_{sweep} \approx 0.57 \left(\frac{\rho_s}{1\,g\,cm^{-3}}\right)\left(\frac{r_p}{1\,km}\right)\left(\frac{a}{R_S}\right) \times \left(\frac{90\,K}{T}\right)^{1/2}\left(\frac{10^5\,g\,cm^{-2}}{\Sigma}\right)\left(\frac{H_p}{H}\right) years \quad (25)$$

We see that making a 1000 km embryo would take $\sim 10^4 H_p/H$ years at Titan, or about ten times longer than it took at Ganymede. Allowing $H_p < H$, the sweep up timescale is always shorter than the drag timescale for $a < 22R_S$. Beyond this distance our model has an optically thin, quiescent disk with $H_p << H$. Therefore, in general, $\tau_{sweep} < \tau_{gas}$. In the inner disk (inside of $20R_S$, $T = 100$ K), where the temperature is inversely proportional to the radial location, the ratio of the sweep up time to the gas drag time is independent of semi-major-axis and particle size $\tau_{sweep}/\tau_{gas} \approx H_p/H$. Since the sweep up times for Saturn are about an order of magnitude longer than for Jupiter, for Saturn there is an increased likelihood that bombardment from outside the Roche-lobe disrupted embryo growth. Furthermore, characteristic embryo sizes < 1000 km are significantly smaller for Saturn's disk. It seems likely that more embryos were lost in the case of Saturn, which might explain the absence of large satellites inside of Titan's orbital radius where collisional events might have been energetic enough to breakup satellite embryos (Greenberg *et al.* 1977). It must be mentioned, however, that weaker turbulence for Saturn than Jupiter might change this conclusion. Nevertheless, a simple model yields similar turbulent viscosities for Saturn and Jupiter (see Figure 4) so it is unclear how important this is. Furthermore, while weaker turbulence may speed up the formation of satellite embryos, it may actually slow down the formation of full size satellites. This is because satellites complete their accretion by drift of satellitesimals, which are bigger and drift slower in the case of weak turbulence. Hence weaker turbulence may actually lower the chances of satellite survival for two reasons. First, because weaker turbulence means that the gas surface density remains close to its original value (see Paper II). Second, because weaker turbulence may lead to longer satellite accretion times. In any event, there are a number of alternative explanations for the absence of large Saturnian satellites inside Titan (see Paper II).

Now we calculate the size of an embryo that will be effective at capturing satellitesimals of mass m_1 drifting across its feeding zone. At Titan we find $m_d \sim 3.5 \times 10^{24}$, which corresponds to ~ 820 km (compared to ~ 1500 km at Ganymede), and a feeding zone of $l_d \sim 2.9 \times 10^4$ km. It took an m_1 satellitesimal 0.6 years (compared to 0.22 years at Ganymede) to cross the embryo's feeding zone For $H_p = H$, it will take 1.3×10^4 years to build an embryo of size ~ 820 km (compared with ~ 2700 years at Ganymede to form an embryo of size ~ 1500 km). Decreasing the gas density by a factor of 4 leads to an embryo size of ~ 410 km (compared to 760 km for the same solid concentration factor for Ganymede). However, such small embryos may be vulnerable to breakup by hypervelocity impacts.

Given that the satellite formation time is the embryo accretion time plus the drift accretion time of embryos, we obtain a time of $10^4 - 10^5$ years for Titan (compared with $10^3 - 10^4$ years for Ganymede).

6.1 Formation of Iapetus

It should be clear by now that we view Iapetus as an analog to Callisto in the sense that it formed on a long timescale from the materials in the outer disk of its primary. In this regard, it is intriguing to note that some of the surface features in Iapetus, such as Cassini Regio, might have a similar coating as Callisto (Denk *et al.* 1999). Aside from its size, there is one way, however, in which Iapetus is markedly different from Callisto; namely, its low density ~ 1.0 g cm^{-3}. This low density makes it unlikely that the dark, reddish material that can be seen on Iapetus was directly incorporated from the solar nebula. Though such material is a component of many bodies in the outer solar system, direct accretion would have led to a larger density for this object (McKinnon 1999). We speculate that the reason for the low density of Iapetus is that for the low gas density of Saturn's envelope the source of the material in Saturn's outer disk came from the ablation of water and methane ice of infalling planetesimals and/or most of the dust settled deeper in before the disk was formed. If so, assuming cosmic mixture for the outer disk may not be valid in this case. Still, the uncertainty in the model leads us to continue to use it (but note that the minimum mass subnebula model has $\sim 200 M_{Iapetus}$ in the outer disk).

The timescale for formation of Iapetus varies significantly

depending on the specific model chosen for the surface density in Saturn's outer disk. For the sake of specificity, here we choose the model that yields enough condensables for just one Iapetus mass from $60R_S$ to $200R_S$ (see Figure 2).

As has been done before we first calculate the characteristic masses (for the dashed curve in Figure 2, Iapetus model). In Saturn's outer disk at $\sim 70R_S$ with $\Sigma_s \sim 1.3$ g cm^{-2} and $\rho_s = 1$ g cm^{-3} (which is the density of Iapetus), we obtain $m_1 \sim 1.3 \times 10^{11}$ g, which corresponds to a satellitesimal radius of ~ 0.03 km and $l_1 \sim 1.8$ km. The embryo size is $m_2 \sim 3.7 \times 10^{21}$ g, which corresponds to a embryo radius of ~ 96 km and $l_2 \sim 5.5 \times 10^3$ km.

At this location the size of an embryo that will capture a significant fraction of the satellitesimals of mass m_1 that drift by is $m_d \sim 1.6 \times 10^{24}$ g, which corresponds to a radius of $\sim$ 720 km and $l_d \sim 7.8 \times 10^4$ km. As was the case with Callisto, however, the satellitesimal will grow due to rubble and dust sweep up as it crosses the embryo's feeding zone (assuming $\bar{\rho}_p \approx \rho_g$). Therefore, the above estimates need to be corrected to take into account that the drift times increase as the satellitesimal grows. Then we obtain $m_d \sim 1.2 \times 10^{24}$ g, which corresponds to a radius of ~ 670 km and $l_d \sim 7.2 \times 10^4$ km. Assuming $\bar{\rho}_p \approx \rho_g$, it will take about 3.4×10^5 years to grow an embryo of that size by dust and rubble sweep-up at that location. It is interesting to note that $m_2 << m_d \lesssim M_{Iapetus}$. A model with 4 times less gas density leads to an embryo size of ~ 350 km at Iapetus.

To complete the accretion of Iapetus we need to accumulate several embryos. Since the timescale for drift of a 500 km embryo at Iapetus' location is $10^6 - 10^7$ years (see Figure 6b), we take this value to be the formation timescale for Iapetus.

6.2 Formation of Hyperion

The origin of Hyperion in the 4:3 mean-motion resonance with Titan presents a significant challenge. A tidal origin of resonance capture as may apply to Galilean satellites (Malhotra and Dermott 1990) seems unlikely to apply to the case of Titan and Hyperion. Given Titan's size and distance from Saturn, significant expansion of its orbit would require Saturn's dissipation parameter Q to be much lower than the lower limit set by the proximity of Mimas. Lee and Peale (2000) concluded that Hyperion could have formed with its present orbital properties from the accretion of satellitesimals in a 4:3 resonance provided that (a) there was a steep gradient ($\propto r^{-3}$) of disk and particles densities, (b) Titan grew to its present size and eccentricity on a timescale of $10^4 - 10^5$ years, and (c) no particles are added to the outside of the disk. Given that our model puts Hyperion in the transition region of the gaseous disk where one would naturally expect steep density gradients (*i.e.* the steep density gradient would result from the edge of the inner disk, not from global disk properties), we find that Lee and Peale's model requirements agree very well with our general satellite formation scenario. We note that these authors found gas drag to be necessary in order to induce satellitesimal orbital decay and capture into resonance.

It might appear that condition (c) is inconsistent with our model but we argue otherwise. Particles from the outer, low density disk would start arriving well after Hyperion's accretion was already complete, and would be composed of a sparse population of rather sizeable objects (tens to hundreds of kilometers). Whether this can account for the Hyperion's irregular shape we defer for future study.

We now check to see whether proto-Titan may capture satellitesimals into resonance in the gas regime corresponding to its accretion. The threshold mass such that proto-Titan can halt the inward migration of a satellitesimal in the vicinity of a $j+1:j$ resonance is given by (Malhotra 1993)

$$\mu_{TH} = \left(\frac{M_S}{M_P}\right)_{TH} = \frac{2}{C_{ad}} \frac{a}{j(j+1)} (\eta v_K \tau_{gas})^{-1} \quad (26)$$

where M_S is the mass of the satellite, M_P is the mass of the planet, and $C_{ad} = C'_{ad}/(1+\eta/e^*) \lesssim 3.3$ is a numerical constant. As in Malhotra (1993), we make the assumption that in the strongly damped regime the quantity $(1+\eta/e^*)$ is roughly constant with forced eccentricity $e^* \sim \eta$. In terms of our model parameters, the threshold mass can be written as

$$\mu_{TH} \simeq \frac{2.9 \times 10^{-3}}{j(j+1)} \left(\frac{1\,g\,cm^{-3}}{\rho_s}\right) \left(\frac{a}{R_S}\right)^{1/2} \times \left(\frac{T}{90\,K}\right)^{1/2} \left(\frac{1\,km}{r_p}\right) \left(\frac{\Sigma}{10^5\,g\,cm^{-2}}\right) \quad (27)$$

which yields $\mu_{TH} \simeq 3.5 \times 10^{-4}$ for a 1 km object for the 4:3 resonance with Titan located at Hyperion ($24.5R_S$), which is near the inner edge of the transition region. Given that Titan satisfies this condition it appears that Hyperion may indeed have been captured in the presence of gas drag. It is possible that Titan migrated inwards over its history. This would place the 4:3 resonance in regions of lower gas density, thus allowing for lower threshold masses. Allowing for a factor of $3-4$ less gas also makes it easier for proto-Titan to capture Hyperion into resonance. Hence Hyperion could well be the result of the accretion of satellitesimals in resonance by proto-Titan as Lee and Peale (2000) have suggested.

For Jupiter we can write

$$\mu_{TH} \simeq \frac{2.3 \times 10^{-3}}{j(j+1)} \left(\frac{1\,g\,cm^{-3}}{\rho_s}\right) \left(\frac{a}{R_J}\right)^{1/2} \times \left(\frac{T}{130\,K}\right)^{1/2} \left(\frac{1\,km}{r_p}\right) \left(\frac{\Sigma}{10^5\,g\,cm^{-2}}\right) \quad (28)$$

which yields $\mu_{TH} \simeq 1.6 \times 10^{-3}$ for a 1 km object for the 4:3 resonance with Ganymede located at $18R_J$. This may indicate that Ganymede did not capture a satellite in resonance because it was not massive enough to stop the inward drag of satellitesimals outside its orbit. However, given that it is

possible to argue in favor of increased solid concentrations, it remains a possibility that Ganymede accreted satellitesimals in resonance which were subsequently lost due to collisions or unstable orbits.

6.3 Formation of Satellites inside of Titan

The first thing to note about the satellites inside of Titan is that by mass they constitute only $\sim$ 3 % of the total mass of the satellite system. The second thing is that they have low densities (Tethys, Enceladus and Mimas have densities consistent with almost all ice, while Rhea is mostly ice [see Table II]) with the sole exception of Dione ($\rho_s \approx 1.5$ g cm^{-3}). The higher density for Dione may reflect a rockier composition or some endogenic process (as evidenced by the observed resurfacing on this satellite but not Rhea) such as cryovolcanism that can close "pores" and lead to larger bulk density. Other factors, such as under-dense ice and the effects of impacts may mar a straightforward interpretation of satellite densities based on composition alone. Nevertheless, it seems likely that as a group these satellites are mostly made of ice. It is also important to note that there is a large gap between the outermost satellite in this group (Rhea at $8.7R_S$) and Titan (at $20R_S$). Lastly, and perhaps most importantly, all large Saturnian satellites (with the sole exception of Iapetus) appear to be sorted according to size, with the smaller satellites further in. We consider this sequence to be significant. We will return to this issue in Paper II.

We expect that these satellites accreted in the presence of significantly less gas than did Titan ($\Sigma \sim 10^4$ g cm^{-2}; see Paper II) about 10^5 years after the end of Saturn's accretion, once the planet cooled enough for water condensation inside the orbit Rhea to take place. Despite their small size, we estimate it took $10^4 - 10^5$ years to accrete these objects.

7 Uranian Satellite System

As we did in the case of Saturn, we begin our discussion of the satellite system of Uranus by noting that here, too, the ratio of masses of the atmospheric envelopes of the primary are roughly consistent with the ratio of masses of the satellite systems. Assuming Saturn to have a $\sim$ 15 Earth mass core and Uranus a smaller $\sim$ 10 Earth mass core, the mass ratio of the envelopes for the two planets is $\sim$ 18. While substantially uncertain, this value compares favorably with the mass ratio of the satellite systems of the two planets $\sim$ 15.

All the regular satellites of Uranus are all well inside Uranus' centrifugal radius located at $\sim 57R_U$. The irregular satellites Caliban and Stephano are found at $280R_U$ and $309R_U$, or approximately $R_{roche}/10$. Inside the centrifugal radius, the main satellites of Uranus are Oberon (at $22R_U$), Titania (at $17R_U$), Umbriel (at $10R_U$), Ariel (at $7R_U$), and Miranda (at $4.9R_U$). As before, it is more meaningful here to establish correspondences between satellites not in terms of planetary radii but in terms of the Hill radius of the planet (see Figure 1). Scaled by the Hill radius of the primary, the location of Oberon corresponds closely to the location of Rhea in Saturn's satellite system. Moreover, the size of Oberon (760 km) is quite similar to the size of Rhea (764 km; though Oberon is denser). Furthermore, there is evidence in the Uranian system of sorting according to size as there is in the Saturnian system. The main difference between the two families of objects is that Saturn's inner satellites are considerably less dense (presumably icier) than Uranus' regular satellites. In fact, of the Uranian satellites only Miranda has a density (1.2 g cm^{-3}) consistent with a object made mostly of ice. It is indeed remarkable that here, too, there is evidence of endogenic activity.

It has been suggested that the satellites of Uranus may have been the byproduct of the impact event that led to its present obliquity (e.g., Pollack *et al.* 1991). However, such a process is unlikely to lead to a sufficiently extended particle disk to produce satellites as far as $22R_U$ (Canup and Ward 2000). Furthermore, the evidence for systematic increases in density and size (see Figure 1) for these satellites is hard to reconcile with an impact origin. Instead, we choose to follow the same general outline to form the satellites of Uranus as we applied to the formation of the regular satellites of Saturn and Jupiter.

A minimum mass model in which the gas disk extends out to the centrifugal radius of the planet at $57R_U$ would set the average gas density at 1.4×10^4 g cm^{-2}. This is quite close to the surface gas density at which the disk becomes optically thin (given gas opacity). In this case, the temperature gradient in the subnebula may not have been sufficiently strong to drive turbulence. So we would expect a cool, largely quiescent disk with gas surface density of $\sim 10^4$ g cm^{-2} as the environment in which the Uranian satellites accreted. This is very similar to the environment we hypothesize led to the inner Saturnian moons (see also Paper II).

In the inner disk, we interpret the gap between the location of the centrifugal radius and the innermost satellite as suggestive of significant satellite migration. In the outer disk, the presence of irregular satellites much closer to the centrifugal radius than is the case for the Jupiter and Saturn satellite systems indicates to us that the outer disk of Uranus did not have enough mass to lead to the formation of regular satellite outside of the centrifugal radius (see also Paper II).

8 Starved Disk Model

A scenario in which the giant planet satellites accrete from a disk produced through the direct infall of gas and solids from a heliocentric orbit has numerous issues to overcome before it can offer an alternative to the model presented here. We list and discuss a few of the outstanding ones, and we leave the development of such a model (if viable) for later work.

The main reason why such a model may be desirable is because it introduces a longer timescale for the formation of the satellites, namely one controlled by the infall of materials from the Roche-lobe. In particular, a "starved" disk might

be used to capture Sun-orbiting planetesimals leading to long assembly times for all the satellites ($\sim 10^6$ years) despite the short accumulation times of the material in the circumplanetary disk $\sim 10^2$ years (Stevenson, personal communication). Because no detailed model of satellite formation in a starved disk scenario has been advanced, we simply discuss some of the issues that any such model has to contend with.

First and foremost is the issue of satellite survival. Recent numerical simulations show that opening a gap does not necessarily terminate accretion of gas onto the planet (Lubow *et. al.* 1999). While at first glance this result may seem welcome news for a model that has the satellite system form after gap opening, it has long been recognized that gas drag (*e.g.* Lunine and Stevenson 1982) makes long term satellite survival in the presence of gas a significant issue. This problem is compounded if one insists in making all the satellites slowly. Doing so deprives this model of the stalling mechanism due to the feedback reaction of the disk that we use (see Paper II) to allow for long term survival. The proto-satellite would never grow to a size that would allow it to stall in the gas disk since it would first drift into the planet. One can postulate the presence of satellite seeds with enough mass to have stalled, but this simply postpones the problem to one of either seed capture or formation. The intrinsic difficulty of any model that relies on the infall of gas after planetary accretion to make the satellite system on a long timescale is that it retains the gas around for a long time.

The alternative is a gas-free accretion model. However, such a model may be difficult to justify. Aside from gas flowing through the gap, another factor contributing to the difficulty of ridding the subnebula of gas is the likelihood that the gas turbulence dies down as the gas becomes optically thin and the planet cools. Hence it is unlikely that gas turbulence alone can lower the gas density in the disk below the value at which the gaseous optical depth is of order unity (unless small dust particles are kept around for a long time, which presents a problem in light of the short coagulation timescales). Also, the locations of the irregular satellites argues for a sharp cut-off in the gas surface density far from the planet. Such a sharp cut-off is inconsistent with strong gas viscosity at that location. Thus, the gas component may stay around until it dissipates due to photodissociation. Furthermore, there are numerous observational reasons why the presence of gas is desirable. We have already touched on a few in this paper, such as the sizes of the Galilean satellites, the capture of Hyperion into resonance, the presence of captured objects at large distances but not closer in, the absence of small satellites far from the planet, and the parity between the mass ratio of atmospheric envelopes of the giant planets and the ratio of mass in their satellite systems; we will follow up on this issue in Paper II.

There is also the issue of the source of the solids. The flow of gas through the gap does not imply flow of solids, since by this time aggregation models (Weidenschilling 1997) lead to mass distributions such that most of the mass of solids is located in objects > 10 km. That is, only a tiny fraction of the mass arriving at Jupiter millions of years after its accretion would be in the form of particulate matter coupled to the gas flowing through the gap. To derive a sufficient amount of such material would require large amounts of gas to flow through, which would make survival of satellitesimals problematic. On the other hand, large planetesimals would not be coupled to the gas, and their dynamics have to be followed independently.

Mosqueira *et al.* (2000) considered Roche-lobe feeding of satellitesimals in tandem with the formation of the regular satellites. To that end, they adapted a symplectic code to treat satellite accretion simultaneously with the feeding of satellitesimals into the planetary environment. The issue arises as to how to capture infalling planetesimals. True capture requires close interaction with material bound in orbit around the planet (which, in a starved disk model, is insufficient to give rise to the observed satellite systems). Even if enough mass were captured to make the satellite systems, this would not guarantee that this mass would end up in the satellite systems. One must make sure not to send most of that material into Jupiter. That is, the disk has to be sufficiently starved to lead to a long formation timescale but its surface density cannot be so low as to decrease the disk capture rate below that of Jupiter (it must be remembered that Jupiter's capture cross section is larger than the planet's physical cross-section). On the other hand, the number density of late arriving planetesimals may not be so high as to send too many planetesimals into the Oort cloud. Thus, such a scenario must be very carefully tuned. Perhaps more importantly, since planetesimals in the outer solar system scatter in million years timescales (Gladman *et al.* 1990), it must be shown that there would be enough planetesimals arriving a million years after the formation of Jupiter to make the Galilean satellites on a long timescale, and still avoid hypervelocity impacts by large planetesimals which might differentiate or even destroy proto-Callisto and breakup all the satellites close to the giant planets. While the delivery of material from the solar nebula to Jupiter probably lasted several million years (Wuchterl *et al.* 2000) the amount of material arriving late is still a small fraction of the total. On a related issue, the late arriving material after the depletion of the nebula gas has been proposed to explain the large core of Neptune (Lissauer *et al.* 1995), but recent work indicates that planetesimals outside of proto-Neptune's feeding zone may evolve along with the planet's orbit and prevent them from colliding with it (Ida *et al.* 2000). While very little material remains exterior to Neptune the issue that concerns us here is the timescale over which this region was cleared of planetesimals.

In addition, lengthening the formation time of the satellites creates a significant problem in that it exposes the proto-satellites to prolonged bombardment from the Roche-lobe, thus substantially decreasing the chances that they will survive. This is particularly problematic for Jupiter, where the velocity of incoming projectiles may be enough to shatter objects as large as $\sim$ 1000 km (Greenberg *et al.* 1977). It is easy to see, then, that forming satellites slowly, out of the mass arriving directly from the Roche-lobe on ballistic orbits may be more likely to destroy than to form satellites. Recall that in our model most satellites (particularly those close to Jupiter)

form quickly, and grow large enough to survive even large impacts (even Callisto grows quickly to embryo size). As a result, a starved disk model may have trouble forming satellites anywhere.

The angular momentum of the satellite system also presents a serious problem to a starved disk model, where most of the mass fed into the system comes in the form of satellitesimals that are not coupled to the gas. Because a swarm of planetesimals is likely to have small net angular momentum with respect to the protoplanet, it is difficult to see how such a swarm can lead to the formation of satellites. Even assuming that satellitesimals are preferentially fed from the outer regions of the solar nebula, one would still be faced with a difficulty avoiding loss of angular momentum during satellite formation (one might even expect preferential capture of retrograde objects as is the case for the irregular satellites). Here again, the long timescale of formation aggravates the situation. This is of particular concern because Jupiter and Saturn both have satellites well outside the centrifugal radius. In our model, the angular momentum of Callisto and Iapetus is ultimately the result of the torque of the Sun on gas flowing into the giant planet from the Roche-lobe. Since the starved disk is fed mostly by large planetesimals uncoupled to the gas, the Sun's torque is not available to this model.

Even if all the above issues are resolved, there is no guarantee that one would end up with satellite systems like those of Jupiter and Saturn. Other issues such a model has difficulties coping with include the low densities of Saturnian satellites other than Titan (especially that of Iapetus), the formation of Hyperion in resonance, the endogenic activity of the small moons of Saturn, the mass to distance relationship in the Uranian and inner Saturnian satellites (see Paper II), the location of the outermost satellite of each planet, the formation of a fully differentiated Ganymede but only a partially differentiated Callisto, and the sizes, positions and densities of the Galilean satellites. Using such a model one may well argue that the compositional gradation among the Galilean satellites is a consequence of impact (Stevenson *et al.* 1986). That is, impacts close to the planet from late arriving high-velocity planetesimals might preferentially re-accrete rock. However, this argument is hard to apply to Saturn, where the satellite density increases fairly systematically out to Titan and then decreases again for Iapetus!

It is possible to argue in favor of a hybrid model in which most of the mass is derived from "late stage" feeding yet one starts with satellite seeds sufficiently massive to avoid some of the issues mentioned above. In that case, it is likely one would resort to the physical processes described in this and in Paper II to accrete and retain such seeds long enough for continued growth to a full size satellite. At this time we do not favor this alternative. First, it is unlikely that such a model can overcome all of the objections listed above. Second, the agreement between the atmospheric envelope mass ratios and satellite systems mass ratios argues against it. Third, although more work needs to be done to verify this claim it seems possible to accrete Callisto partially differentiated without resorting to the feeding of solids through the gap. As we argued before, given our model it is still possible (though this may be unlikely regardless of the model) that particulate matter coupled to the high specific angular momentum gas flowing through the gap after giant planet gap-opening contributes a significant fraction to the mass of moons forming outside the centrifugal radius of the giant planet, thus lengthening their formation timescale. However, a *starved disk* model forms *all* the regular satellites out of late arriving material, whereas the angular momentum of the gas arriving after the giant planet has accreted most of its mass would take it to orbits outside the centrifugal radius (considering the torque of the Sun on the gas that flows into the giant planet).

To close this discussion, we point out that regardless of the details of such a model, it is likely that it would predict a partially differentiated state for Titan. Accretion onto Titan would have occurred even slower, with less energetic impacts, and at a lower temperature (both of the nebula and the object) than Callisto's accretion. Furthermore, a starved disk model would preclude the presence of significant amounts of ammonia in Titan or any other satellite. Therefore, one would expect a partially differentiated (Callisto-like) Titan.

9 Conclusions

We have used a consistent model for the accretion of regular satellites of Jupiter, Saturn and Uranus. Though a variety of accretion scenarios arise out of our model, we argue that this is not tantamount to special pleading for each satellite; rather, the various possibilities all derive from the parameter space available to the model. In our view, the complexity of the model is justified by the observations.

We investigate a model for giant planet regular satellite formation in which the satellites accrete in the presence of a dense inner gaseous disk extending out to the planet's centrifugal radius, and from an extended, low density outer disk extending out to a fraction of the planetary Hill radius. The accretion of the satellites takes place at the tail end of the formation of the giant planet, at a time of heavy Roche-lobe planetesimal bombardment; however, the bulk of the materials in the satellites is derived from condensables left behind by planetesimal break-up in the giant planet's extended, collapsing envelope, from which the circumplanetary gas disk formed. We assume a "minimum mass" model to estimate the mass of the inner disk; and in light of the high-Z enhancement in Jupiter and Saturn, we consider increased solid concentrations by a factor of $3 - 4$. We take the similarity of the reconstituted satellite mass ratio between Jupiter and Saturn (~ 3.7) and the ratio of the atmospheric envelopes of these two planets as an indication that (a) the same general process applied to both of their satellite systems, and (b) the amount of material left in the inner disk is related to amount of gas in the planet's envelope. Therefore, we use the above ratio to estimate the relative mass in the gas disks of the two planets. Similarly, the atmospheric envelope mass ratio between Saturn and Uranus ~ 18 com-

pares well with the ratio of the masses in the satellite systems of these two planets ~ 15. This leads us to use a minimum gas model extending out to Uranus' centrifugal radius (and not to the present location of Oberon, given that the Uranian satellites probably migrated inward) to estimate the amount of gas present in the Uranian inner disk subnebula.

There are three possible mechanisms that can lead to the formation of the extended disk. First is the spin-out scenario of Korycansky *et al.* (1991). Second, gas viscosity may push gas out to large distances. Third, the torque exerted by the Sun on gas flowing through the Roche-lobe at the time of giant planet gap opening, or, more generally, at end of planetary accretion may lead to the formation of an extended disk. The first two mechanisms both rely on dust opacity. In the case of the spin-out model dust opacity is needed to keep Jupiter's envelope sufficiently puffed-up to spin-out as it contracts. On the other hand, gas viscosity may only lead to an extended outer disk if strong gas turbulence lasts a time comparable to the viscous timescale far from the planet; this may only happen if dust keeps the inner gas disk optically thick. Because we expect the dust opacity to decrease sharply over time as a result of dust coagulation, we we favor the third possibility, and base our estimate for the mass of the outer disk on it. To determine the size of the outer disk, we rely on the locations of the irregular satellites of the giant planets. Connecting their location to the size of the disk allows us to explain the lack of irregulars closer to the planet. With this in mind, we expect that the outer disks of Jupiter and Saturn extended out to $\sim R_{roche}/5$, and contained enough condensables to form Callisto and Iapetus respectively.

At present, the best candidate mechanism to generate turbulence with α in the range $10^{-4} - 10^{-2}$ is an entropy gradient in the subnebula leading to a non-barotropic equation of state (Klahr and Bodenheimer, in press). Such a model leads to turbulence that is a function of position and time. Post-accretion, turbulence is likely to die down to α values of $10^{-6} - 10^{-5}$, thus allowing the subnebula to cool down. In particular, regions of the disk with temperature close to the background temperature of the nebula at the location of the primary should be nearly quiescent, with low gas viscosity and long orbital decay times. In this regard, we interpret the cut-off in the distribution of irregular satellites of Jupiter and Saturn as strongly suggestive of a sharp decrease in the outer disk gas density in the neighborhood of $R_{roche}/5$. Such a strong density gradient is consistent with laminar gas flow. On the other end, because the inner disk of the giant planets (except perhaps Uranus) is non-isothermal both radially and vertically, weak turbulence is expected there for as long as the gas remains optically thick (with $\Sigma > 10^4$ g cm^{-2}). Such a turbulence model may remove gas more efficiently close to the planet; and it may have difficulty lowering the gas surface density below the value given above (unless small dust particles are kept around for viscous timescales, despite the comparatively short coagulation timescales), perhaps leading to a flat surface density profile.

Given our subnebula parameters, we show that gas drag dominates migration for particles $< 500 - 1000$ km, and the tidal torque of the gas disk is stronger for larger objects. In the inner disk, dust and rubble are swept up fast enough to form a 1000 km satellite embryo in $< 10^3$ years for Jupiter and $< 10^4$ years for Saturn as long as some settling of the particle layer takes place. This timescale may be sufficiently short for the embryo to survive the effects of gas drag and planetesimal bombardment from the Roche-lobe. Once the embryo reaches $\sim$ 1000 km size it will capture a significant fraction of the satellitesimals that migrate inwards into its feeding zone due to gas drag, making it likely that most of the condensible mass in the disk ends up in the satellite system instead of being lost to the planet. Thus, roughly speaking, a "minimum mass" model may in fact apply to the formation of satellites. We expect that satellites stopped growing when either the disk ran out of accretable materials, or when an outer embryo choked off the growth of proto-satellites inside of its orbit. The latter possibility may explain the sequence of sizes of the Galilean satellites, and the observation that the largest satellites of both Saturn and Jupiter occur just inside the centrifugal radius. While it is possible that for the largest satellites partial vaporization of infalling satellitesimals and subnebula gap opening may have reduced the mass accretion rate, it is unlikely that these processes were able to terminate accretion altogether. Nevertheless, for the largest satellites (Ganymede, Titan and Callisto) gap-opening may have significantly lowered the accretion efficiency of inwardly drifting satellitesimals (a greater proportion of such objects may "horseshoe" past a large satellite surrounded by a gap). Hence the similarity in their masses may be connected with this process. If so, their final masses may not be determined solely by the total amount of mass present outside their orbit and inside the orbit of its outer neighbor. Perhaps more likely, both factors may came into play.

Though our model leads in some cases to long formation times for full-grown satellites, in all such cases the embryos that led to the satellite formed quickly, and the long formation timescale is derived from the slow accretion of dispersed embryos. Our model forms Ganymede in Jupiter's inner disk in $10^3 - 10^4$ years at a temperature of $\sim$ 250 K, and Titan in Saturn's inner disk in $10^4 - 10^5$ years at a temperature of $\sim$ 100 K. The upper bound is computed by estimating the size of the region from which a satellite draws materials, and then computing the timescale for embryos to drag that distance and form the satellite. The lower bound is obtained by assuming that once an embryo grows to a size that it can capture most of the satellitesimals that drift into its feeding zone, its growth accelerates. In the case of Titan and Ganymede, we speculate that this accretion took place fast enough that these satellites avoided significant inward migration. Thus, we would expect that the embryo which led to their formation originated from the neighborhood of the centrifugal radius of each of their planets. Though the lower gas surface gas density in Saturn's system probably led to a longer formation timescale for Titan, our model predicts that this satellite accreted too fast to avoid runaway differentiation.

In the outer disk, the low temperature of the gas ($\sim$ 130 K

for Jupiter and $\sim$ 90 K for Saturn) leads us to expect that it is characterized by weak turbulence driven only by the vertically thin particle layer shear (Cuzzi *et al.* 1993). Therefore, despite the longer dynamical times and low solid surface densities, the timescale for the formation of embryos by dust and rubble sweep up and by drift augmented accretion of satellitesimals is about 100 times faster than the orbital decay timescales for such embryos. Consequently, we expect embryos to form quickly until the disk becomes depleted of dust and rubble. Continued growth of similarly sized embryos will take place at the Safronov timescale and lead to sizes of several hundred kilometers in a timescale comparable to their drift times. Once these embryos reach the position of proto-Callisto most of them will be accreted by it. We calculate characteristic embryo sizes by comparing the drift times of satellitesimals across twice the embryo's feeding zone to the synodic time of two objects separated by half that distance. In our model Callisto's accretion timescale is set by the inward drift of embryos $300 - 500$ km (with the smaller embryo size the result of the longer satellitesimal drift time of a model with 4 times greater concentration of solids) from as far away as $\sim 150 R_J$ (compared with $\sim 23 R_J$ for Ganymede). Similarly, the timescale for the accretion of Iapetus is set by the drift of embryos from as far as $\sim 200 R_S$. We also show that the Safronov timescale to build embryos $\lesssim$ 500 km at distances $\sim 100 R_J$ is about 10^6 years. Furthermore, the orbital decay time of such an object from that distance is also $\sim 10^6$ years (though the timescale depends on the concentration of solids in the disk).

A formation timescale of $\sim 10^6$ years for Callisto (and $10^6 - 10^7$ years for Iapetus) may be slow enough to lead to a partially differentiated state for Callisto (Iapetus is made of ice) consistent with the two layer model advanced by Anderson *et al.* (2001), which has a clean ice layer $\sim$ 300 km overlying a mixed ice and rock-metal interior. It must be stressed that although this model leads to large embryos hitting the proto-satellite, they do so at the escape velocity of the proto-satellite (as supposed to the hypervelocity impacts that would result from Roche-lobe objects). In this energy regime, crater diameters are roughly $\sim 3 r_s$, so that the penetration depth of such objects are likely on the order of their radius, with excavation depths being even smaller (Melosh 1989). Thus, a single collision may not lead to runaway differentiation of the proto-satellite. While impacts with embryos of hundreds of kilometers will bury heat, it will also overturn the upper layers of a satellite, perhaps allowing it to cool faster. Furthermore, larger solid concentrations will decrease the size of the embryos while lengthening the timescale of formation. It is also possible (though probably unlikely given Iapetus' low density, and the low solid content expected to couple to the gas at late times) that particulate matter coupled to high specific angular momentum gas flowing through the gap after giant planet gap-opening lengthens the timescale of formation of regular satellites *outside* the centrifugal radius. Still, more work needs to be done to check whether our model can realistically lead to a partially differentiated Callisto.

Callisto could then be said to be the result of slowly assembling hundreds to thousands of "cold" embryos. This may account for the preferential retention of ices more volatile than water in Callisto than in Ganymede. This also means that (possibly unlike Ganymede and Titan) both Callisto and Iapetus are likely to have migrated large distances (see Paper II for an explanation of their present day locations). Lewis (1974) hypothesized that lower formation temperatures for Callisto than for Ganymede would likely have led to the accretion of solid ammonia hydrate in Callisto. Our model indeed has Callisto forming cold; however, it does so in a region of the disk disconnected from the inner, optically thick region. Therefore, we expect Callisto bulk composition to adhere closely to solar mixtures. In the case of Iapetus, we speculate that the bulk of its material was derived by the ablation of ices from planetesimals that hit Saturn's envelope and/or water enriched material as a result of dust settling in the envelope, which might explain this satellite's low density.

Given our model, Titan's methane atmosphere may still be the result of the condensation of methane clathrate hydrate (Lewis 1974). Another interesting if somewhat speculative possibility of our model is that Titan out-gassed its atmosphere as a result of a collision with an Iapetus-sized object. Given its location, it is unlikely that Iapetus collected all the material in Saturn's outer disk. Therefore, large embryos could have formed outside the centrifugal radius which ultimately ended up colliding with Titan. Iapetus itself may owe its dark, reddish material to the condensation of methane in the subnebula.

Since our model has an optically thick inner disk, it is also possible that ammonia is responsible for ancient volcanic plains in Tethys and Dione. In the inner disk one might expect production and outward transport of ammonia. However, the outer regions of the disk would not be affected. The lack of any resurfacing in Callisto and its presence in the much smaller Dione seems to indicate that Callisto lacks ammonia but Dione has it. Given our model, it is possible that ammonia is responsible for the ancient volcanic plains in Tethys and Dione. But it must be pointed out that Rhea appears inert. It might be that Rhea received less ammonia than Dione by virtue of its location. On the other hand, it is also possible that ammonia fails to resurface larger satellites. There is also the issue of the D/H ratio for the satellites. While more work has to be done in this respect, to the extent that neither Callisto nor Iapetus was coupled to a thick subnebula one might expect an enhanced D/H ratio for these satellites with respect to Ganymede and Titan. However, given Iapetus location Titan probably received a substantial amount of material from the outer disk in the late stages of its accretion. Hence it may not be surprising that the measured D/H ratio in Titan's atmosphere is comparable to that of comet Halley. It is unclear whether Ganymede's D/H ratio can be expected to be substantially lower than that of Callisto, but the issue merits further study. Finally, we point out that whereas Callisto is likely to have accreted homogeneously (its accretion time is longer than the disk cooling time at its location) the same may not be true for Ganymede or Titan. It must be stressed that despite the different predictions that our model makes for satellites forming in the inner and outer disks, the basic processes that led to their formation are essentially the same.

Because Saturn's disk is characterized by longer dynamical times and has less gas spread out over a larger distance than Jupiter's disk, our model leads to significantly longer accretion timescales for the satellites of Saturn. It is possible that no large satellites formed inside of Titan because the embryo formation timescale $\sim 10^4$ years made them vulnerable to hypervelocity impacts close to the planet (but see Paper II for alternative explanations based on satellite migration). This mechanism may work because characteristic embryos in Saturn's disk are small (< 1000 km).

We have seen that our model has Ganymede and Titan forming in the inner disk, and Callisto and Iapetus in the outer disk. It also has Hyperion forming in the transition region. This is significant because it fits well with the formation model of Lee and Peale (2000), which has Hyperion captured into resonance by proto-Titan in the presence of a strong gas density gradient. Given our subnebula parameters, we show that Titan satisfies the criterion for gas drag capture of kilometer sized satellitesimals into resonance, whereas Ganymede does not. This may explain the presence of Hyperion at Titan's 4:3 resonance location, and the absence of a corresponding small satellite in resonance with Ganymede (though such an object may have formed in an unstable orbit and been subsequently scattered, or been lost due to collisions). Furthermore, Callisto may have formed in a region of the disk where the gas drag was weak enough that typical satellitesimal eccentricities were larger than the critical value such that resonance capture probability becomes small, leaving the transition region between the outer and inner disks of the giant planets as the only place where resonant capture is likely. If so, this may place significant constraints on the environment that gave rise to regular satellites of giant planets. This issue merits further work.

We extend this model to the satellites of Uranus. Though for Uranus the mass for the inner or outer disks may not have been enough to form a Titan or an Iapetus, we find remarkable similarities between the Uranian satellite system and the inner Saturnian satellites. We defer further discussion of this issue to Paper II. Here we simply point out that we interpret the gap between the centrifugal radius and the outermost Uranian regular satellite as suggestive of substantial satellite migration inwards. In the outer disk, our model ties the absence of a regular satellite outside the centrifugal radius to the presence of irregulars close to the centrifugal radius (compared to the irregulars of Jupiter and Saturn).

The question of the silicate fraction of the satellites is likely to be quite complicated with many thorny issues which are beyond the scope of this paper (see McKinnon *et al.* 1997 for a review). Here we simply point out that our model seems to fit better with the view that most of the regular satellites of giant planets are not water deprived but water enriched. By this we mean that regular satellites forming in regions of the subnebula where water condensation had taken place probably had more water available to them than given by solar mixtures, even if they lost some of that water in the process of accretion. As has been done before (e.g. Podolak *et al.* 1993), we note that all the regular satellites of giant planets with the exception of Io and Europa have silicate fractions well below those of Triton, Pluto and Charon (though at least Triton may have lost a significant amount of water during its history). There are at least four mechanisms that can lead to water enrichment, and we suggest that their interplay may have the best chance of explaining the observed silicate fractions of the regular satellites of the giant planets. First, ice ablation of planetesimals hitting the envelope of the giant planet and/or dust settling can add water content to satellites forming far from the planet (this may have played a major role in the case of Iapetus and to a lesser extent in the case of Callisto). Second, more water may be available under nebular conditions applicable to satellites forming in the inner disk (this may apply to Ganymede, Titan and to a lesser degree the Uranian satellites). Third, non-homogeneous accretion may lead to selective loss of silicates (this may be applicable to the inner Saturnian satellites and perhaps to Miranda; see Paper II). However, much more work will have to be done to check this possibility.

We briefly consider the alternative conceptual model that Callisto's timescale was set by the timescale over which solids were fed into the system, and that all the regular satellites of Jupiter and Saturn formed from a "starved disk". We conclude that this scenario faces significant hurdles. Nevertheless, the issue needs to be settled. We propose that a good test of this alternative model is whether or not Titan is differentiated. Our model leads us to the conclusion that while Titan took considerably longer to form than Ganymede, it still formed in a short timescale ($< 10^5$ years), making it very likely that it is fully differentiated. On the other hand, the "starved disk" model implies a long accretion time for Titan with lower temperatures and slower impacts (compared to Callisto), and small quantities of NH_3 present. While it may be possible to avoid this conclusion by fine tuning parameters such as the size of the impactors, we suggest that such a model would predict a partially differentiated (Callisto-like) Titan. The Cassini mission is likely to resolve this issue conclusively.

ACKNOWLEDGEMENTS

We would like to thank Jeffrey Cuzzi, Kevin Zahnle, Doug Lin, Peter Bodenheimer and Jeff Moore for discussions. One of us (I. M.) had numerous very helpful discussions with Dave Stevenson. We also thank Jeffrey Cuzzin, Kevin Zahnle, and Jack Lissauer for reading the manuscript and suggesting improvements. This research was supported by the NRC and a grant from the Planetary Geology and Geophysics program.

Appendix A: Velocity Dispersion in the Outer Disk

Because of the effects of gas drag, we expect the outer disk will be populated by similar-sized embryos; smaller objects would be quickly incorporated into larger objects by drift augmented accretion. Given this, we ask what is the velocity dispersion of these objects. The mean eccentricities e and inclinations i are determined by the balance between excitation due to mutual encounters and damping due to gas drag and/or collisions. Using the average time rate of change of e and i

determined by Adachi *et al.* 1976 (their equation 4.15), as well as their mean-square variations (Hayashi *et al.* 1977, equation 5.24), we have

$$\frac{de^2}{dt} = \frac{0.47}{\tau_{cg}} \frac{1}{i\sqrt{i^2+e^2}} - \frac{2e^2}{\tau_g}(0.77e + 0.64i + \eta) - \frac{e^2}{\tau_c} = 0 \quad (A1)$$

$$\frac{di^2}{dt} = \frac{0.094}{\tau_{cg}} \frac{1}{i\sqrt{i^2+e^2}} - \frac{i^2}{\tau_g}(0.77e + 0.85i + \eta) - \frac{i^2}{\tau_c} = 0 \quad (A2)$$

where the characteristic timescales due to gas τ_g, physical collisions τ_c, and gravitational collisions τ_{cg} are given by

$$\tau_g = \frac{16\rho_s r_p c a^2}{3C_D G M_P \Sigma} \quad (A3)$$

$$\tau_c = \frac{1}{\sqrt{2}n\sigma u} \quad (A4)$$

$$\tau_{cg} = \frac{3M_P^2}{36.64\pi^2 a^2 \Omega \Sigma_s \rho_s r_p^3 \ln \Lambda_r} \quad (A5)$$

where n is the number density of particles, $\sigma = 4\pi r_p^2(1+\Theta)$ is the cross-section with $\Theta = v_{esc}^2/2u^2$ the Safranov parameter, $u^2 = \langle e^2 + i^2 \rangle v_K^2/2$ is the mean-square velocity, and

$$\Lambda_r = \frac{\langle e^2 + i^2 \rangle M_P}{4am_s} s = \frac{\langle e^2 + i^2 \rangle M_P u}{8\pi a \Omega \Sigma_s r_p^2} \quad (A6)$$

with the mean free path $s = 2\rho_s r_p u/3\Omega\Sigma_s$. We find solutions for the cases in which interactions are balanced by (a) gravitational collisions, (b) physical collisions, and (c) both physical and gravitational collisions. For these solutions we assume that $\eta << e, i$, but we note that this may be only marginally true. The first case has already been found by Hayashi *et al.* and is given by

$$e = 1.7i = 0.78(\tau_g/\tau_{cg})^{1/5} \quad (A7)$$

We find that for a 500 km satellitesimal at $a = 150\,R_J$ with a density of $\rho_s = 1.5$ g cm^{-3}, $e \sim 0.17$ and $i \sim 0.1$. For case (b) in which we balance interactions with physical collisions only, we also find a simple relationship

$$e = \sqrt{5}i = 0.99(\tau_c/\tau_{cg})^{1/4} \quad (A8)$$

Here for the same 500 km object at $a = 150\,R_J$, we find that $e \sim 0.23$ and $i \sim 0.1$. However, for case (c) we cannot decouple the characteristic times from equations (A1) and (A2) in order to find a simple relationship between e and i. We find that a good estimate that encompasses the sizes of satellitesimals we are interested in for the outer disk to be

$$e \sim 1.9i \sim 0.83(\tau_g/\tau_{cg})^{1/5}(1.1 + \tau_g/2e\tau_c)^{-1/5} \quad (A9)$$

In this case for a 500 km object at $a = 150\,R_J$, we find that $e \sim 0.16$ and $i \sim 0.084$.

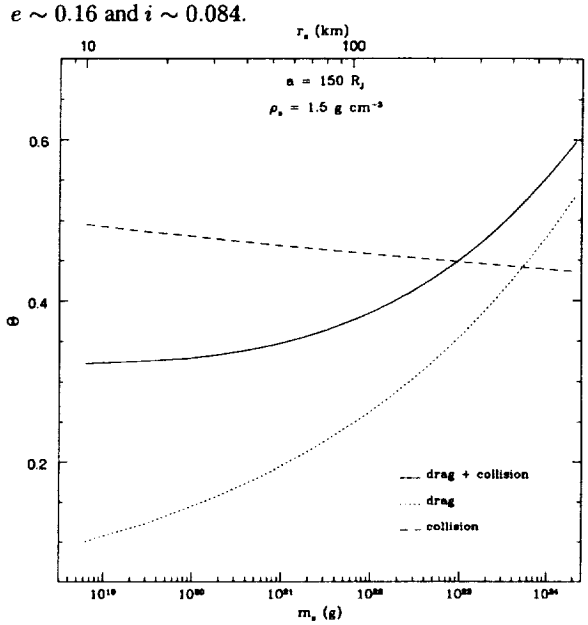

Figure 7: Safronov parameter plotted versus both satellitesimal mass and radius (assuming $\rho_s = 1.5$ g cm^{-3}) for three cases in the outer disk. Mutual encounters are balanced by physical collisions (dashed curve), gravitational collisions (dotted curve), and both gravitational and physical collisions (solid curve). For this wide range of satellitesimal sizes, the $\Theta < 1$ indicating gravitational focusing is unimportant.

In all three cases, we must iterate to find solutions for e and i, and the focusing factor given by $F_g = 1 + \Theta$. We have solved these three cases for a range of satellitesimal mass at $a = 150\,R_J$ and plotted them versus the Safranov parameter in **Figure 7**. The satellitesimals are assumed to have a density of $\rho_s = 1.5$ g cm^{-3}. The dashed line represents the solution to case (a). The Safranov parameter actually decreases as one approaches higher masses. This is due to the fact that there are fewer physical collisions for larger particles. The dotted line corresponds to case (b) where we balance the pumping of e and i with gravitational collisions. Here Θ increases as one approaches larger masses. Likewise case (c), which combines both effects, corresponds to the solid line. Physical collisions dominate for the smaller masses, while gas drag wins out for larger particles as the number of physical collisions decrease.

For all cases we find $\Theta < 1$ indicating that over this range of satellitesimal sizes the focusing is weak. Interestingly, the ratio of drag time τ_{gas} to collision time τ_c can be written as

$$\frac{\tau_{gas}}{\tau_c} \sim 6\left(\frac{e}{i}\right)\left(\frac{130\,K}{T}\right)^{3/2}\left(\frac{150\,R_J}{a}\right)^{3/2}. \quad (A10)$$

Notice that this is independent of particle size. Also note that since $e/i \approx constant$ this is independent of the velocity dispersion. Likewise, the Safronov accretion timescale is independent of velocity dispersion for $F_g \sim 1$.

Appendix B: Collisional Breakup of Satellitesimals

Sufficiently large impacts, even occurring at velocities close to the escape velocity of the target, have the potential for fragmentation of the original body. The outcome of such impacts are most often characterized by a dimensionless parameter

$$f_1 = A\left(\frac{E_{disr}}{E_p}\right)^b \qquad (B1)$$

where E_{disr} is the "disruption energy" of the target, E_p is the impact energy imparted by the projectile, A is a constant of order unity, and $b \sim 0.8 - 1.25$ for various target materials (*e.g.* Fujiwara *et al.* 1977; Melosh 1989; Davis *et al.* 1999). The parameter f_1 is the ratio between the mass of the largest fragment due to the collision, and the mass of the original body. For $f_1 \simeq 1$, the collision leads to erosion of the target, for $f_1 \simeq 0.5$ the target has suffered a "significant breakup" (threshold of catastrophic disruption), and $f_1 \ll 1$ indicates a catastrophic breakup of the target into small fragments (Melosh 1989). The disruption energy of the target is generally taken to be a function of the target's strength Y only, however for large objects one must consider the self-gravity effects of the target, which we may express for spherical objects with uniform mass as

$$E_{disr} \sim \frac{4}{3}\pi r_s^3\left[c_1 Y + \frac{4}{3}c_2\pi G\rho_s^2 r_s^2\right] \qquad (B2)$$

where c_1 and c_2 are dimensionless constants of order unity. The crossover size such that the strength of the target is on the same order as its gravitational binding energy has been found to range from several 100 km radii to as small as a few 100 m (Ahrens and Love 1996). Assuming $c_1 = c_2 = 3/5$ (gravitational binding energy coefficient) in equation (B2), one finds that the transition size may be expressed as $r_s \sim (3Y/4\pi G\rho_s^2)^{1/2}$, which yields objects tens of kilometers in size for strengths in the MPa range.

As an example, we consider the collision of two equally-sized objects ($r_s > 100$ km) in the outer disk assuming that target strength is unimportant. The energy imparted into the target is taken to be half of the total collisional kinetic energy $E_p = m_p v_p^2(1 + 2\Theta)/4 \approx m_p v_{esc}^2/2$ where we assume the remaining half of the energy remains in the projectile. The Safronov parameter is taken to be $\Theta = 0.5$ as a representative value (see Figure 7). We find that $f_1 \simeq 0.5 - 0.7$ which satisfies the criterion for partial disruption of the the target. This suggests that collisional disruption may have played an important role in determining the accretion timescale for satellite embryos in the outer disk.

References

ADACHI, I., C. HAYASHI, AND K. NAKAZAWA 1976. The gas drag effect on the elliptic motion of a solid body in the primordial solar nebula. *Prog. Theor. Phys.* **56**, 1756-1771.

AHRENS, T. J., AND S. G. LOVE 1996. Strength versus gravity dominance in catastrophic impacts. *Lun. Plan. Sci.* **27**, 1-2.

ANDERSON, J. D., G. SCHUBERT, R. A. JACOBSEN, E. L. LAU, W. B. MOORE, W. L. SJOGREN 1998. Distribution of rock, metals, and ices in Callisto. *Science* **280**, 1573-1576.

ANDERSON, J. D., R. A. JACOBSON, T. P. MCELRATH, W. B. MOORE, G. SCHUBERT, AND P. C. THOMAS 2001. Shape, Mean Radius, Gravity Field, and Interior Structure of Callisto. *Icarus* **153**, 157-161.

BALBUS, S. A., AND J. F. HAWLEY 1991. A powerful local shear instability in weakly magnetized disks. II. Nonlinear evolution. *Astrophys. J.* **376**, 223.

BALBUS, S. A., J. F. HAWLEY, AND J. M. STONE 1996. Nonlinear stability, hydrodynamical turbulence, and transport in disks. *Astrophys. J.* **467**, 76.

BELL, K. R., P. M. CASSEN, H. H. KLAHR, T. HENNING 1997. The Structure and Appearance of Protostellar Accretion Disks: Limits on Disk Flaring. *Astrophys. J.* **486**, 372-387.

BRYDEN G., X. CHEN, D. N. C. LIN, R. P. NELSON, AND C. B. PAPALOIZOU 1999. Tidally induced gap formation in protostellar disks: Gap clearing and suppression of protoplanetary growth. *Astrophys. J.* **514**, 344-367.

CAMERON, A. G. W., AND M. R. PINE 1973. Numerical models of the primitive solar nebula. *Icarus* **18**, 377-406.

CAMERON, A. G. W. 1978. Physics of the primitive solar nebula and of giant gaseous protoplanets. In *Protostars and Planets* (T. Gehrels ed.) pp. 453-487, Univ. of Arizona Press, Tucson.

CANUP, R. M., AND W. R. WARD 2000. A possible impact origin of the Uranian satellite system. Proceedings of the 32nd DPS meeting, 2000.

CARLSON, R. W. 1999. A tenuous carbon dioxide atmosphere on Jupiter's moon Callisto. *Science* **283**, 820-821.

CASSEN, P., AND D. PETTIBONE 1976. Steady accretion of a rotating fluid. *Astrophys. J.* **208**, 500-511.

CASSEN, P., AND A. MOOSMAN 1981. On the formation of protostellar disks. *Icarus* **48**, 353-376.

CASSEN, P., AND A. SUMMERS 1983. Models of the

formation of the solar nebula. *Icarus* **53**, 26-40.

CHIANG, E. I., AND P. GOLDREICH 1999. Spectral energy distributions of passive T Tauri disks: Inclination. *Astrophys. J.* **519**, 279.

CORADINI, A., P. CERRONI, G. MAGNI, AND C. FEDERICO 1989. Formation of the satellites of the outer solar system - Sources of their atmospheres. In *Origin and Evolution of Planetary and Satellite Atmospheres* (S. K. Atreya, J. B. Pollack, and M. S. Matthews, Eds.), pp. 723-762, Univ. of Arizona Press, Tucson.

CORADINI, A., C. FEDERICO, AND G.MAGNI 1981. Gravitational instabilities in satellite disks and formation of regular satellites. *Astr. Ap.* **99**, 255-261.

CORADINI, A., C. FEDERICO, AND P. LUCIANO 1982. Ganymede and Callisto: Accumulation heat content. In *The Comparative Study of Planets* (A. Coradini and M. Fulchignoni, Eds.) D. Reidel, Dordrecht.

CUZZI, J. N., A. R. DOBROVOLSKIS, AND J. M. CHAMPNEY 1993. Particle-gas dynamics in the midplane of a protoplanetary nebula. *Icarus* **106**, 102-134.

DAVIS, D. R., P. FARINELLA, AND F. MARZARI 1999. The missing Psyche family: Collisionally eroded or never formed?. *Icarus* **137**, 140-151.

DENK, T., G. NEUKUM, R. JAUMANN, T. ROATSCH, K. S. NOLL, C. C. PORCO, AND S. W. SQUYRES 1999. Iapetus – Summary of recent work, prospects for Cassini. LPSC XXX.

FRIEDSON, A. J., AND D. J. STEVENSON 1983. Viscosity of rock-ice mixtures and applications to the evolution of icy satellites. *Icarus* **56**, 1-14.

FUJIWARA, A., G. KAMIMOTO, AND A. TSUKAMOTO 1977. Destruction of basalt bodies by high-velocity impact. *Icarus* **31**, 277-288.

GAMMIE, C. F. 1996. Linear theory of magnetized, viscous, self-gravitating gas disks. *Astrophys. J.* **463**, 725.

GLADMAN, B., AND M. DUNCAN 1990. On the fates of minor bodies in the outer solar system. *Astron. J.* **100**, 1680-1693.

GOLDREICH, P. AND S. TREMAINE 1978. The formation of the Cassini division of Saturn's rings. *Icarus* **34**, 240-253.

GOLDREICH, P. AND S. TREMAINE 1979. The excitation of density waves at the Lindblad and corotation resonances by an external potential. *Astrophys. J.* **233**, 857-871.

GOLDREICH, P., N. MURRAY, P. Y. LONGARETTI, AND D. BANFIELD 1989. Neptune's story. *Science* **245**, 500-504.

GOODMAN, J., AND B. PINDOR 2000. Secular instability and planetesimal formation in the dust layer. *Icarus* **148**, 537.

GREENBERG, R., D. R. DAVIS, W. K. HARTMANN, AND C. R. CHAPMAN 1977. Size distribution of particles in planetary rings. *Icarus* **30**, 769-779.

HAYASHI, C., K. NAKAZAWA, AND I. ADACHI 1977. Long-term behavior of planetesimals and the formation of the planets. *Pub.Astr.Soc.Japan* **29**, 163-196.

HIBBITTS, C. A., R. PAPPALARDO, J. KLEMASZEWSKI, T. B. MCCORD, AND G. B. HANSEN 2001. Comparing carbon dioxide distributions on Ganymede and Callisto. Proceedings of the 32nd LPSC, Houston 2001.

IDA, S., BRYDEN, G., LIN D. N. C., AND H. TANAKA. Orbital migration of Neptune and orbital distribution of trans-Neptunian objects. *Astrophys. J.* **534**, 428-445.

JULIAN, W. H., AND A. TOOMRE 1966. Non-axisymmetric responses of differentially rotating disks of stars. *Astrophys. J.* **146**, 810-832.

KARY, D. M., J. J. LISSAUER, AND Y. GREENSZWEIG 1993. Nebular gas drag and planetary accretion. *Icarus* **106**, 288.

KLAHR, H., AND P. BODENHEIMER 2001. Turbulence in accretion disks. The global baroclinic instability. Astronomische Gesellschaft Abstract Series, vol. 18, JENAM 2001, September 10-15, 2001, Munich, Germany.

KORYCANSKY, D. G., J. B. POLLACK, AND P. BODENHEIMER 1991. Numerical models of giant planet formation with rotation. *Icarus* **92**, 234-251.

KORYCANSKY, D. G., AND J. C. B. PAPALOIZOU 1996. A method for calculations of nonlinear shear flow: Application to formation of giant planets in the solar nebula. *Astrophys. J. Suppl.* **105**, 181-190.

LEE, M. H., AND S. J. PEALE 2000. Making Hyperion. Presented at the 32nd DPS meeting, American Astronomical Society, October 2000.

LEWIS, J. S. 1972. Low temperature condensation from the solar nebula. *Icarus* **16**, 241-252.

LEWIS, J. S. 1974. The temperature gradient in the solar nebula. *Science* **186**, 440-443.

LI, H., J. M. FINN, R. V. E. LOVELACE, AND S. A. COLGATE 2000. Rossby wave instability of thin accretion disks. II. Detailed linear theory. *Astrophys. J.* **533**, 1023-1034.

LIN, D. N. C. 1981. Convective accretion disk model for the primitive solar nebula. *Astrophys. J.* **246**, 972-984.

RICHARDSON, D. C., T. QUINN, J. STADEL, AND G. LAKE 2000. Direct large-scale N-body simulations of planetary dynamics. *Icarus* **143**, 45-59.

RUDEN, S. P., AND D. N. C. LIN 1986. The global evolution of the primordial solar nebula. *Astrophys. J.* **308**, 883-901.

RYU, D., AND J. GOODMAN 1992. Convective instability in differentially rotating disks. *Astrophys. J.* **388**, 438-450.

SAFRONOV, V. S. 1969. *Evolution of the protoplanetary cloud and formation of the Earth and planets.* Nauka, Moscow. [Transl.: Israel Program for Scientific Translations, 1972. NASA TTF-677.

SCHUBERT, G., D. J. STEVENSON, AND K. ELLSWORTH 1981. Internal structures of the Galilean satellites. *Icarus* **47**, 46-59.

STEVENSON, D. J., A. W. HARRIS, AND J. I. LUNINE 1986. Origins of satellites. In *Satellites* (J. A. Burns and M. S. Matthews, Eds.) Univ. of Arizona Press, Tucson.

STEVENSON, D. J. 2001. Jupiter and its Moons. *Science* **294**, 71-72.

TAKEUCHI, T., S. M. MIYAMA, AND D. N. C. LIN 1996. Gap formation in protoplanetary disks. *Astrophys. J.* **460**, 832.

WARD, W. R. 1993. Density waves in the solar nebula: Planetesimal velocities. *Icarus* **106**, 274-287.

WARD, W. R. 1996. Planetary accretion.Proceedings of the Astronomical Society of the Pacific, vol. **107**, (T. W. Rettig and J. M. Hahn, Eds.) pp. 337-361.

WARD, W. R. 1997. Protoplanet migration by nebula tides. *Icarus* **126**, 261-281.

WEIDENSCHILLING, S. 1974. A model for accretion of the terrestrial planets. *Icarus* **22**, 426-435.

WEIDENSCHILLING, S. 1984. Evolution of grains in a turbulent solar nebula. *Icarus* **60**, 553-567.

WEIDENSCHILLING, S. 1988. Formation processes and timescales for meteorite parent bodies. In *Meteorites and the Early Solar System* (J. F. Kerridge and M. S. Matthews, Eds.) Univ. of Arizona Press, Tucson.

WEIDENSCHILLING, S. 1997. The origin of comets in the solar nebula: A unified model. *Icarus* **127**, 290-306.

WEIDENSCHILLING, S., AND J. N. CUZZI 1993. Planetesimal formation in the protoplanetary nebula. In *Protostars and Planets* (T. Gehrels Ed.) Univ. of Arizona Press, Tucson.

WETHERILL, G. W. 1980. Formation of the terrestrial planets. *Ann. Rev. Astron. Astrophys.* **18**, 77-113.

WUCHTERL, G., GUILLOT T., AND J. J. LISSAUER, 2000. In *Protostars and Planets IV*, V. Mannings, A. Boss, S. Russell, Eds. (Univ. of Arizona Press, Tucson, AZ, 2000), pp. 1081-1109.

LIN, D. N. C., AND J. PAPALOIZOU 1980. On the structure and evolution of the primordial solar nebula. *Mon. Not. Roy. Astron. Soc.* **191**, 37-48.

LIN, D. N. C., AND J. PAPALOIZOU 1993. On the tidal interaction between protostellar disks and companions. In *Protostars and Planets III* (E. H. Levy and J. I. Lunine Eds.), pp. 749-836. Univ. of Arizona, Tucson.

LISSAUER, J. J. 1995. Urey Prize Lecture: On the Diversity of Plausible Planetary Systems. *Icarus* **114**, 217-236.

LISSAUER, J. J., POLLACK, J. B., WETHERILL, G. W., AND D. J. STEVENSON 1995. In Neptune and Triton, ed. M. S. Matthews and A. M. Schumann (Tucson: Univ. Arizona Press), 37.

LISSAUER, J. J., AND G. R. STEWART 1993. Growth of planets from planetesimals. In *Protostars and Planets III* (E. H. Levy and J. I. Lunine Eds.), pp. 1061-1088. Univ. of Arizona, Tucson.

LOVELACE, R. V. E., H. LI, S. A. COLGATE, AND A. F. NELSON 1999. Rossby wave instability of keplerian accretion disks. *Astrophys. J.* **513**, 805-810.

LUBOW, S. H., M. SEIBERT, AND P. ARTYMOWICZ 1999. Disk accretion onto high-mass planets. *Astrophys. J.* **526**, 1001.

LUNINE, J. I. 1989. Primitive bodies: Molecular abundances in comet Halley as probes of cometary formation environments. In *The Formation and Evolution of Planetary Systems* (H. A. Weaver, F. Paresce, and L. Danly, Eds.), pp. 213-242, Cambridge Univ. Press, Cambridge.

LUNINE, J. I., AND D. J. STEVENSON 1982. Formation of the Galilean satellites in a gaseous nebula. *Icarus* **52**, 14-39.

LYNDEN-BELL, D. AND J. E. PRINGLE 1974. The evolution of viscous disks and the origin of the nebula variables. *Mon. Not. Roy. Astron. Soc.* **168**, 603-637.

MALHOTRA, R., AND S. F. DERMOTT 1990. The role of secondary resonances in the orbital history of Miranda. *Icarus* **85**, 444-480.

MALHOTRA, R. 1993. Orbital resonances in the solar nebula: Strengths and weaknesses. *Icarus* **106**, 264-273.

MCKINNON, W. B., SIMONELLI D. P., AND G. SCHUBERT 1997. Composition, internal structure, and thermal evolution of Pluto and Charon. In *Pluto and Charon* (S. A. Stern, D. J. Tholen. Eds.), pp. 295, The University of Arizona Press, Tucson.

MCKINNON, W. B. 1999. Midsize icy satellites. In *The New Solar System* (J. Kelly Beatty, C. C. Peterson, A. Chaikin. Eds.), pp. 297, Sky Publishing Co., Cambridge.

MELOSH, H. J. 1989. *Impact Cratering: A Geological Process*. Oxford Univ. Press, New York.

MOORE, J. M., E. ASPHAUG, D. MORRISON, J. R. SPENCER, C. R. CHAPMAN, B. BIERHAUS, R. J. SULLIVAN, F. C. CHUANG, J. E. KLEMASZEWSKI, R. GREELEY, K. C. BENDER, P. E. GEISSLER, P. HELFENSTEIN, AND C. B. PILCHER 1999. Mass movement and landform degradation on the icy Galilean satellites: Results of the Galileo nominal mission. *Icarus* **240**, 294-312.

MOSQUEIRA, I., P. R. ESTRADA, AND J. E. CHAMBERS 2000. Satellitesimal feeding and the formation of the regular satellites. Proceedings of the 32nd DPS meeting, 2000.

PODOLAK, M., W. B. HUBBARD, AND J. B. POLLACK 1993. Gaseous accretion and the formation of the giant planets. In *Protostars and Planets III* (E. H. Levy and J. I. Lunine Eds.), pp. 1061-1088. Univ. of Arizona, Tucson.

POLLACK, J. B., A. S. GROSSMAN, R. MOORE, AND H. C. GRABOSKE, JR. 1976. The formation of Saturn's satellites and rings as influenced by Saturn's contraction history. *Icarus* **29**, 35-48.

POLLACK, J. B., A. S. GROSSMAN, R. MOORE, AND H. C. GRABOSKE, JR. 1977. A calculation of Saturn's gravitational contraction history. *Icarus* **30**, 111-128.

POLLACK, J. B., J. A. BURNS, AND M. E. TAUBER 1979. Gas drag in primordial circumplanetary envelopes: A mechanism for satellite capture. *Icarus* **37**, 587-611.

POLLACK, J. B., J. LUNINE, AND W. C. TOTTEMORE 1991. Origin of the Uranian satellites. In *Uranus* (J. T. Bergstralh, E. D. Miner, and M. S. Matthews, Eds.) Univ. of Arizona Press, Tucson.

POLLACK, J. B., D. HOLLENBACH, S. BECKWITH, D. P. SIMONELLI, T. ROUSH, AND W. FONG 1994. Composition and radiative properties of grains in molecular clouds and accretion disks. *Astrophys. J.* **421**, 615-639.

PRINN, R. G., AND B. FEGLEY JR. 1981. Kinetic inhibition of CO and N_2 reduction in circumplanetary nebulae: Implications for satellite composition. *Astrophys. J.* **249**, 308-317.

PRINN, R. G., AND B. FEGLEY JR. 1989. Solar nebula chemistry: Origin of planetary, satellite, and cometary volatiles. In *Origin and Evolution of Planetary and Satellite Atmospheres* (S. K. Atreya, J. B. Pollack, and M. S. Matthews, Eds.), pp. 78-136, Univ. of Arizona Press, Tucson.